https://doi.org/10.5194/tc-2020-155
Preprint. Discussion started: 3 July 2020

The Cryosphere Discussions
Open Access
EGU

Heterogenous CO_2 and CH_4 content of glacial meltwater of the Greenland Ice Sheet and implications for subglacial carbon processes

Andrea J. Pain[1,2], Jonathan B. Martin[1], Ellen E. Martin[1], Shaily Rahman[1,3]

[1] University of Florida, Department of Geological Sciences, Gainesville, FL 32611
[2] Now at: University of Maryland Center for Environmental Science, Horn Point Lab, Cambridge, MD 21613
[3] Now at: University of Southern Mississippi, Department of Marine Science, Stennis Space Center, MS 39529

Correspondence to: Andrea J. Pain (ajpain@ufl.edu)

Abstract. Accelerated melting of the Greenland Ice Sheet (GrIS) has increased freshwater delivery to the Arctic Ocean and amplified the need to understand the impact of GrIS meltwater on Arctic greenhouse gas (GHG) budgets. We measured carbon dioxide (CO_2) and methane (CH_4) concentrations and $\delta^{13}C$ values and use geochemical models to evaluate subglacial CH_4 and CO_2 sources and sinks in water discharging from three subglacial outlets of the GrIS in southwest (Isunnguata and Russell Glaciers) and southern Greenland (Kiattut Sermiat). CH_4 concentrations vary by orders of magnitude between sites and are saturated with respect to atmospheric concentrations at Kiattut Sermiat, but are supersaturated at southwest sites, even though oxidation reduces concentrations by up to 50% during periods of low discharge. CO_2 concentrations range from supersaturated at Isunnguata to undersaturated at Kiattut Sermiat. CO_2 is consumed by mineral weathering throughout the melt season at all sites, however differences in the magnitude of subglacial CO_2 sources result in meltwaters that are either sources or sinks of atmospheric CO_2. The predominant source of CO_2 at Isunnguata is organic matter (OM) remineralization, but Russell and Kiattut Sermiat sites have multiple or heterogeneous subglacial CO_2 sources that maintain atmospheric CO_2 concentrations at Russell but not at Kiattut Sermiat where CO_2 is undersaturated. These results highlight the variability in GHG dynamics under the GrIS. Constraining this variability will improve our understanding of the impact of GrIS melt on Arctic GHG budgets, as well as the role of continental ice sheets in GHG variations over glacial-interglacial timescales.

1 Introduction

Glaciers play an important role in global chemical cycles due to the production of fine-grained sediments that participate in carbonate and silicate mineral weathering reactions (Table 1), which are the principal sink of atmospheric CO_2 over geologic timescales (Berner et al., 1983; Walker et al., 1981). Variations in the weathering intensity of comminuted sediments may contribute to glacial-interglacial atmospheric CO_2 variations as sediments are alternately covered by ice and exposed following ice retreat. However, the importance of CO_2 consumption by mineral weathering is poorly understood, including effects from the advance and retreat of continental ice sheets (Ludwig et al., 1999). Recent evaluations of carbon budgets in proglacial environments indicate that mineral weathering results in net sequestration of atmospheric CO_2, suggesting

https://doi.org/10.5194/tc-2020-155
Preprint. Discussion started: 3 July 2020

that proglacial systems are underrecognized as Arctic CO_2 sinks (St. Pierre et al., 2019), however alternate processes could lead to the production of greenhouse gases (GHG) in glacial systems. For instance, CH_4 production in anaerobic subglacial environments driven by the remineralization of organic matter (OM) contained in soils and forests covered during glacial margin fluctuations has been suggested as a potential carbon feedback to drive warming (Sharp et al., 1999; Wadham et al., 2008). Because the global warming potential of CH_4 is 25 times greater than CO_2, even limited subglacial methanogenesis has the potential to strongly impact the GHG effect of glacial meltwater. Combined inorganic and organic subglacial processes may therefore produce glacial meltwater that is a source or sink of GHG. While the net impact of these processes on modern carbon fluxes is poorly constrained, determining these impacts will improve modern carbon budgets as well as depictions of how fluxes may have evolved during the advance and retreat of continental ice sheets.

In subglacial environments where remineralization is limited by low OM availability, the major element solute load of glacial meltwater is typically dominated by products of mineral weathering reactions (Tranter, 2005). The extent of mineral weathering in subglacial environments depends in part on the availability of acids to drive reactions, namely sulfuric and carbonic acids (Table 1). Sulfuric acid is derived from the oxidation of reduced sulfur species, which largely occur as iron-sulfide minerals including pyrite (Tranter, 2005). Sulfide oxidation may occur abiotically, however the kinetics of microbially mediated sulfide oxidation is several orders of magnitude faster and may lead to local depletion of oxygen provided sufficient supply of sulfide minerals (Sharp et al., 1999). In contrast, carbonic acid may be derived from multiple external or *in situ* sources of CO_2 to the system. The dominant external source is supraglacial meltwater that flows to the subglacial system through moulins following equilibration with atmospheric CO_2 (Fig. 1). Unlike proglacial environments where free exchange between water and the atmosphere may resupply CO_2 consumed by weathering, subglacial environments may be partially or fully isolated from the atmosphere, limiting further atmospheric CO_2 invasion and thus the extent of mineral weathering with carbonic acid. However, additional atmospheric CO_2 may be delivered in open portions of the subglacial environment though exchange in fractures or moulins along subglacial flow paths or in partially air-filled conduits, allowing a much greater magnitude of carbonic acid mineral weathering (Graly et al., 2017). CO_2 may also be derived from *in situ* sources, such as gaseous CO_2 contained in ice bubbles of basal ice, or fluid inclusions in rocks that release volatiles (including CO_2) following mechanical grinding (Macdonald et al., 2018). When OM is available, its remineralization also generates CO_2 (and potentially CH_4) along with nutrients, but low OM availability in many subglacial systems limits remineralization as a CO_2 source (Fig. 1).

The role of subglacial carbon processes may play an increasingly important role in modern Arctic carbon budgets as disproportionate warming increases glacial meltwater and sediment fluxes to the ocean, particularly from the Greenland Ice Sheet (GrIS). The Greenland Ice Sheet (GrIS) is the last remaining ice sheet in the Northern hemisphere following collapse of all others since the Last Glacial Maximum (~25 ka). It has been losing mass at increasing rates that averaged 286±20 Gt/yr between 2010-2018, representing a six-fold increase since the 1980s (Mouginot et al., 2019). While mineral weathering significantly modifies the composition of GrIS subglacial discharge (e.g. Hindshaw et al., 2014; Deuerling et al., 2018; Urra

https://doi.org/10.5194/tc-2020-155
Preprint. Discussion started: 3 July 2020

et al., 2019) and should consume CO_2 similar to other glacial and proglacial environments, the recent identification of microbially driven reactions (including methanogenesis) in subglacial environments of the GrIS indicates that organic processes may also play a role (Dieser et al., 2014; Lamarche-Gagnon et al., 2019; Musilova et al., 2017). The relative importance of subglacial GHG sinks (CO_2 consumption through mineral weathering) and sources (such as OM remineralization) determine the GHG composition of subglacial discharge, which may then serve as a source or a sink of atmospheric GHGs. Constraining the relative impacts and variability of these processes underneath the GrIS will provide important information regarding the current and future impact of GrIS loss on Arctic carbon budgets, as well the role of continental ice sheets on carbon cycle feedbacks.

To evaluate the net impact of carbon processes on the GHG composition of subglacial discharge of the GrIS, we compare water chemistry, dissolved CO_2 and CH_4 concentrations, and gas stable isotopic compositions between three subglacial discharge sites draining land-terminating glaciers of the GrIS over the melt seasons of 2017 and 2018 (Fig. 2). We employ mass balance models utilizing the concentrations of major cations and anions to determine the magnitude of the impact on CO_2 concentrations from mineral weathering reactions (Table 1). These results are combined with measured gas concentrations to determine the relative importance of mineral weathering compared to OM remineralization on the CH_4 and CO_2 content of subglacial discharge. We also assess the temporal and spatial variability of these processes under the GrIS to improve our understanding of carbon cycling in Greenland subglacial environments and the implications of GrIS mass loss on Arctic carbon budgets.

2 Methods

2.1 Study locations

Our three subglacial discharge locations are located in southwest (Fig. 2a, b) and southern (Fig. 2a, c) Greenland. The Isunnguata Glacier (IS; 67°09'27.1" N, 50°03'25.0" W) and Russell Glacier (RU; 67°05'22.1" N, 50°14'18.7" W) drain to the Watson River, which is one of the largest proglacial rivers in Greenland. Watson River discharge is monitored by PROMICE (Programme for Monitoring of the Greenland Ice Sheet; van As et al., 2018) and total discharge was 4.3 and 3.6 km^3 of water in 2017 and 2018, respectively (van As et al., 2018). The total catchment size for the Isunnguata is 15,900 km^2, though our water samples were collected from a smaller sub-catchment with a drainage area of approximately 40 km^2 (Lindbäck et al., 2015; Rennermalm et al., 2013). The total drainage area for the Russell glacier is estimated at 300 km^2. This estimate comes from subtracting the Leverett drainage area estimated at approximately 600 km^2 (Hawkings et al., 2016) from the approximately 900 km^2 catchment that includes the Russell and Leverett drainages (Lindback et al., 2015). While discharge from the third site in southern Greenland, Kiattut Sermiat (KS; 61°12'13.5" N, 45°19'49.1"W), is not monitored, a previous study using dye tracing techniques estimated approximately 0.22 km^3 of discharge in 2013, and its catchment size was estimated at 36 km^2 (Hawkings et al., 2016). Underlying lithologies differ between sites. Watson River sites are located near the boundary between the Archean Craton to the south and the southern Nagssugtoqidian Orogen to the north (Henriksen et

https://doi.org/10.5194/tc-2020-155
Preprint. Discussion started: 3 July 2020

al., 2009). The Archean block is composed of granites and granulite facies orthogneisses that were intruded by mafic dykes during Paleoproterozoic rifting. These rocks were deformed and modified during subsequent continent-to-continent collision in the Paleoproterozoic to create the amphibolite facies gneisses of the southern Nagssugtoqidian Orogen (van Gool et al., 2002). Kiattut Sermiat lies within the Paleoproterozoic Ketilidian fold belt (Henriksen et al., 2009). Lithologies in this region include the Julianehåb Granite and associated basic intrusions and the sedimentary and volcanic rocks of the Mesoproterozic Gardar Province that include a suite of alkaline igneous rocks and basaltic dykes with interbedded sandstones (Kalsbeek and Taylor, 1985; Upton et al., 2003).

Previous studies have characterized chemical weathering reactions in subglacial discharge to the Watson River (Deuerling et al., 2018; Hasholt et al., 2018; Yde et al., 2014), Kiattut Sermiat (Hawkings et al., 2016), and comparatively between these sites (Urra et al., 2019). There has been extensive work regarding ice sheet dynamics and hydrology in the Watson River catchment (Van As et al., 2017, 2018; Lindbäck et al., 2015) as well as Kiattut Sermiat (Warren and Glasser, 1992; Winsor et al., 2014). Previous studies near these study locations have identified CH_4 and CO_2 supersaturation in subglacial discharge of the Isunnguata site (Christiansen and Jørgensen, 2018; Ryu and Jacobson, 2012), while methanogenic microbial communities have been observed at Russell Glacier (Dieser et al., 2014) and CH_4 supersaturation at the Leverett Glacier (Lamarche-Gagnon et al., 2019), which also flows into the Watson River (Fig. 2c). Subglacial permafrost has been identified near the Isunnguata site (Ruskeeniemi et al., 2018) and attributed to Holocene fluctuations in the ice sheet margin. While a similar Holocene ice retreat and re-advance may have occurred in southern Greenland (Larsen et al., 2016), it is unknown whether this retreat led to the formation of organic deposits.

2.2 Sample collection

We collected water samples from subglacial discharge sites in spring and fall of 2017, and the summer of 2018 to observe seasonal variations in water composition. Samples were collected as close as possible to the subglacial discharge site, which was less than 10 m for the Isunnguata site, approximately 100 m for the Russell glacier site, and approximately 1.1 km for the Kiattut Sermiat site (Fig. 2). We collected water samples by pumping water through a 0.5-cm flexible PVC tube that was placed in flowing water as far as possible from shore (approximately 1-2 m). A YSI Pro-Plus sensor that was calibrated daily was installed in an overflow cup filled from the bottom to measure specific conductivity (Sp.C), temperature, pH, dissolved oxygen, and oxidation-reduction potential (ORP). These parameters were monitored until stable, between about 10 and 30 minutes, after which samples were collected and preserved in the field according to the solute to be measured after being filtered through a 0.45 µm trace-metal grade Geotech high capacity disposable canister filter. Samples for cations and anions were collected in HDPE bottles; cation samples were preserved with Optima-grade ultrapure nitric acid (pH<2) while no preservative was added to anion samples. Samples for ammonium (NH_4) were filtered into 15 mL polypropylene containers and frozen until analysis. Dissolved inorganic carbon (DIC) samples were filtered through 0.2 µm filters directly to the bottom of 20 ml Qorpac glass vials and allowed to overflow until sealed tightly with no headspace.

https://doi.org/10.5194/tc-2020-155
Preprint. Discussion started: 3 July 2020

Gas samples were collected in duplicate via headspace extractions according to methods outlined in Repo et al. (2007) and Pain et al. (2019). Unfiltered water was pumped into the bottom of 500 mL bottles until they overflowed. Bottles were immediately capped with rubber stoppers fitted with two 3-way inlet valves. 60 mL of water was extracted from one inlet and replaced with 60 mL of atmospheric air (for spring and fall 2017 sampling trips) or ultrapure N_2 gas in a gas bag (summer 2018 sampling trip). Bottles were shaken for 2 minutes to equilibrate headspace gas with water, and headspace gas was extracted and immediately injected into 60 ml glass serum bottles that had been evacuated immediately prior to sample introduction. Samples were stored at room temperature until analysis, which occurred within one week of collection. Measured headspace concentrations were converted to dissolved concentrations using methods outlined in Pain et al. (2019). When atmospheric air was used for headspace extractions, atmosphere samples were collected in tandem and analyzed to correct each sample for calculated dissolved CO_2 and CH_4 concentrations and isotopic compositions. This correction altered CH_4 concentrations by up to 22% for one sample from the Russell glacier, though less than 5% for all other samples, and resulted in a correction of δ^{13}C-CH_4 of up to 1.3‰. For CO_2, the correction altered concentrations by up to 15% for one sample collected at Kiattut Sermiat, though less than 10% for all other samples, and resulted in a correction of δ^{13}C-CO_2 of up to 0.4‰.

For fall 2017 and summer 2018 sampling trips, alkalinity was measured in the field laboratory within 3 days of collection by titration with 0.01 N HCl using the Gran method. Because alkalinity measurements were not available for the spring 2017 sampling trip, we estimate alkalinity with PHREEQc modeling and the phreeqc.dat database (Parkhurst, 1997) using major cations and anions, pH, temperature, and DIC concentrations as model inputs.

2.3 Laboratory analysis

Gas samples were analyzed for CO_2 and CH_4 concentrations, and δ^{13}C-CO_2 and δ^{13}C-CH_4 on a Picarro G2201-i cavity ring-down spectrometer. Carbon isotopic compositions are reported in reference to Vienna Pee Dee Belemnite (VPDB). Check standards of known CO_2 and CH_4 concentrations and isotopic compositions were measured during each sample run and were accurate within 10%. Anion and cation concentrations were measured on an automated Dionex ICS-2100 and ICS-1600 Ion Chromatograph, respectively. Error on replicate analyses was less than 5%. DIC concentrations were measured on a UIC (Coulometrics) 5011 CO_2 coulometer coupled with an AutoMate Preparation Device. Samples were acidified and the evolved CO_2 was carried through a silver nitrate scrubber to the coulometer where total C was measured. Accuracy was calculated to be ±0.1 mg/L based on measurement of check standards. Dissolved ammonium (NH_4) concentrations were analyzed on a Seal AutoAnalyzer III. Error on check standards was less than 10%.

2.4 Methane modeling

To assess CH_4 sources and sinks, we calculate ε_c, or the carbon isotopic fractionation factor between CO_2 and CH_4 as defined in Whiticar (1999):

$$\varepsilon_c = \delta^{13}C_{CO2} - \delta^{13}C_{CH4} \quad (5)$$

https://doi.org/10.5194/tc-2020-155
Preprint. Discussion started: 3 July 2020

Values of ε_c reflect methanogenesis pathways (acetoclastic or CO_2 reduction) as well as the extent of oxidation. Values of ε_c between approximately 40 and 55‰ are produced for CH_4 produced via acetoclastic methanogenesis, while CO_2 reduction produces values between approximately 55 and 90‰. Lower values (ε_c between 5 and 30) result when CH_4 oxidation predominates. Modern atmospheric input without additional alteration of CO_2 or CH_4 isotopic systematics results in a ε_c value of approximately 40 (Whiticar, 1999).

We calculated CH_4 oxidation using the isotopic method outlined in Mahieu et al. (2008) and Preuss et al. (2013). The fraction of oxidized methane (f_{ox}) in an open system is given by:

$$f_{ox} = \frac{\delta_E - \delta_P}{1000 \cdot (\alpha_{ox} - \alpha_{trans})} \quad (6)$$

where δ_E is the measured $\delta^{13}C\text{-}CH_4$ value for each water sample, δ_P is $\delta^{13}C\text{-}CH_4$ of produced methane, α_{ox} is the oxidation fractionation factor, and α_{trans} is a fractionation factor resulting from diffusive transportation of CH_4. While the exact value of δ_P is unknown, diagenetic alteration of $\delta^{13}C\text{-}CH_4$ values through oxidation or transport only enrich $\delta^{13}C\text{-}CH_4$ signatures, therefore the value of δ_P is taken as the most depleted $\delta^{13}C\text{-}CH_4$ signature assuming it is the least impacted by diagenetic alteration. Literature-reported values for α_{ox} range between 1.003 and 1.049. We calculate the fraction of oxidized methane with the largest fraction factor (α_{ox} = 1.049; Mahieu et al., 2008), which yields the minimum amount of CH_4 oxidation required to explain the observed variations in $\delta^{13}CH_4$, and thus is a conservative estimate for CH_4 oxidation. Literature-reported values for α_{trans} vary from 1 for advection-dominated systems to 1.0178 for diffusion-dominated porous media (Visscher et al., 2004; Mahieu et al., 2008; Preuss et al., 2013). We assume that transport is advection dominated and thus assume α_{trans} = 1.

2.5 Mineral weathering and carbonate modeling

We used major cation and anion concentrations and alkalinity to partition solutes into the four mineral weathering reactions in Table 1 after correcting solute concentrations for marine aerosol deposition using measured chloride concentrations and standard seawater element ratios. The mass balance model followed the methods of Deuerling et al. (2019). After apportioning solutes to mineral weathering reactions, we used the stoichiometries of reactions to calculate the impact of each reaction on dissolved CO_2 concentrations (Table 1). The mineral weathering model apportions solutes to reactions in Table 1 based on the ratios of Ca/Na and Mg/Na in silicate minerals in stream bedload samples, which were taken to be 0.54 and 0.38, respectively, for Isunnguata and Russell Glacier samples (Deuerling et al., 2019; Hindshaw et al., 2014; Wimpenny et al., 2010, 2011) and 0.39 and 0.27, respectively, for Kiattut Sermiat samples (Da Prat and Martin, 2019). Because mineral weathering reactions may both add and remove CO_2, we discuss both the net impact of mineral weathering on CO_2 concentrations (Net $CO_{2\text{-}MW}$), which may have a positive or negative value:

$$[\text{Net } CO_{2\text{-}MW}] = [CO_{2\text{-}CarbCA}] + [CO_{2\text{-}CarbSA}] + [CO_{2\text{-}SilCA}] \quad (7)$$

as well as the total impact of mineral weathering on CO_2 concentrations (Total $CO_{2\text{-}MW}$),

https://doi.org/10.5194/tc-2020-155
Preprint. Discussion started: 3 July 2020

$$[\text{Total } CO_{2\text{-MW}}] = |[CO_{2\text{-CarbCA}}]| + |[CO_{2\text{-CarbSA}}]| + |[CO_{2\text{-SilCA}}]| \quad (8)$$

where changes in the concentrations of CO_2 are defined by their absolute values. To discuss the relative importance of individual reactions, we define proportional contributions of each reaction as follows:

$$\%CO_{2\text{-CarbCA}} = \frac{|[CO_{2-CarbCA}]|}{[Total\ CO_{2-MW}]} * 100 \quad (9a)$$

$$\%CO_{2\text{-CarbSA}} = \frac{|[CO_{2-CarbSA}]|}{[Total\ CO_{2-MW}]} * 100 \quad (9b)$$

$$\%CO_{2\text{-SilCA}} = \frac{|[CO_{2-SilCA}]|}{[Total\ CO_{2-MW}]} * 100 \quad (9c)$$

We combine measured CO_2 concentrations with Net $CO_{2\text{-MW}}$ in order to determine the magnitude of CO_2 production or consumption in the subglacial environment due to processes besides mineral weathering. This analysis assumes that the concentration of CO_2 measured at the subglacial outlet is equivalent to the net change in CO_2 due to mineral weathering plus the sum of all other subglacial CO_2 sources and sinks. We refer to the sum of all other subglacial CO_2 sources and sinks as $CO_{2\text{-total}}$, which represents the amount of CO_2 that must have been supplied to the subglacial environment to balance the mineral weathering CO_2 sink:

$$CO_{2\text{-measured}} = \text{Net } CO_{2\text{-MW}} + CO_{2\text{-total}} \quad (10)$$

The sources of CO_2 to $CO_{2\text{-total}}$ may be evaluated through the use of Keeling plots, which are constructed as the inverse of CO_2 concentrations ($[CO_2]^{-1}$) versus stable isotopic composition ($\delta^{13}C\text{-}CO_2$). If variations in the concentration and isotopic composition of CO_2 arise from the mixing of two CO_2 reservoirs with constant isotopic compositions and concentrations (Keeling, 1958), a linear relationship is expected between $[CO_2]^{-1}$ and $\delta^{13}C\text{-}CO_2$. The y-intercept of a regression between these variables represents the isotopic composition of the high-CO_2 end member. Because measured CO_2 concentrations include both subglacial CO_2 sources and sinks, which may include considerable consumption through mineral weathering reactions, the magnitude of the total subglacial CO_2 source is taken as $CO_{2\text{-total}}$. We therefore construct Keeling plots between $[CO_{2\text{-total}}]^{-1}$ and measured $\delta^{13}C\text{-}CO_2$ values because while mineral weathering impacts the concentration of CO_2, its isotopic composition is not appreciably altered (Myrttinen et al., 2012) compared to the range of isotopic compositions of potential CO_2 end members, namely OM remineralization, atmospheric CO_2, and lithogenic CO_2 sources due to mechanical grinding (Fig. 1).

2.6 Discharge relationships

We evaluate the relationship between subglacial CH_4 and CO_2 dynamics and discharge using discharge records provided by PROMICE (Programme for Monitoring of the Greenland Ice Sheet; van As et al., 2018). Discharge records are collected at the outlet of the Watson River, which represents the combined discharge of Isunnguata and Russell glaciers as well as other outlet glaciers including the Leverett Glacier and major tributaries including the Orkendalen River (Fig. 2).

https://doi.org/10.5194/tc-2020-155
Preprint. Discussion started: 3 July 2020

Watson River discharge estimates are therefore greater than the true discharge of our individual sampling locations, however we assume that discharge at the Isunnguata and Russell subglacial outlet sites is roughly proportional to Watson River discharge and exhibits similar temporal variability (Rennermalm et al., 2012). Because diurnal fluctuations in river discharge can be large, and differing water travel times from subglacial outlet sites to the Watson River mouth induces a lag of up to 8 hours between maximum daily discharge at subglacial discharge sites and the Watson River outlet, we compare subglacial CH_4 and CO_2 concentrations to average daily discharge, calculated as the average of hourly discharge estimates over the days on which subglacial discharge water samples were collected. Because no discharge information is available for Kiattut Sermiat, we assess discharge relationships at Watson River (Isunnguata and Russell) sites only.

3 Results

3.1 Temporal variability in water chemistry and gas concentrations

Chemical parameters differ between subglacial discharge sites as well as throughout the melt season. Specific conductivity (Sp.C; Fig. 3a) is typically highest at Kiattut Sermiat (26±8 µS/cm), followed by Russell (22±5 µS/cm) and Isunnguata sites (13±9 µS/cm; Fig. 3a). All sites show variability throughout the melt season, with lowest values occurring in the summer for Isunnguata and Russell, while Sp.C drops continuously throughout the melt season for KS. Sites differ in pH, and values at Kiattut Sermiat (8.2±0.4) are higher than both Russell (7.2±0.2) and Isunnguata (6.6±0.6; Fig. 3b), and while values vary throughout the melt season, no consistent trend is identified between sites. The saturation of dissolved oxygen (D.O.) with respect to atmospheric concentrations is similar between sites, though Isunnguata (98±8%) values fall below Russell (115±16%) and Kiattut Sermiat (117±11%) during all sampling times and exhibit undersaturation in the mid-summer, while Russell and Kiattut Sermiat are consistently supersaturated (Fig. 3c). Alkalinity is similar at Russell (93±31 µeq/L) and Kiattut Sermiat (93±26 µeq/L) which are higher than at Isunnguata (39±25 µeq/L), but all reach minimum values in summer (Fig. 3d). CH_4 concentrations differ by orders of magnitude between sites (Fig. 3e) and are consistently supersaturated with respect to atmospheric concentrations at Isunnguata (648±411 ppm or 1575±997 nM) and Russell (58±33 ppm or 110±78 nM), while close to atmospheric equilibrium at Kiattut Sermiat (4±2 ppm or 9±5 nM). $\delta^{13}C\text{-}CH_4$ values (Fig. 3f) are similar between Isunnguata (-54.7±7.5‰), Russell (-52±7.3‰), and Kiattut Sermiat (-57.6±14.2‰). Measured CO_2 concentrations (Fig. 3g) are consistently supersaturated with respect to atmospheric concentrations for Isunnguata (685±230 ppm or 58±18 µM), near atmospheric equilibrium for Russell (442±31 ppm or 29±4 µM) and undersaturated for Kiattut Sermiat (263±33 ppm or 19±2 µM). $\delta^{13}C\text{-}CO_2$ values (Fig. 3h) are lower in spring and fall for Isunnguata (-16.6±4.0‰) compared to Russell (-13.7±2.3‰) and Kiattut Sermiat (-16.1±1.6‰) sites, though similar seasonal variation occurs for all sites with relatively more depleted values in the spring and fall compared to summer.

https://doi.org/10.5194/tc-2020-155
Preprint. Discussion started: 3 July 2020

245 **3.2 Methane oxidation and relationship with discharge**

Values of ε_c are similar throughout the melt season for Isunnguata (38±10‰) and Russell (38±9‰) and are relatively higher in the summer sampling period, while Kiattut Sermiat ε_c values are higher on average (42±13‰; Fig. 4a) with lowest values in the summer. Estimates of f_{ox} are similar between Isunnguata (17±15%), Russell (23±15%), and Kiattut Sermiat sites (25±22%; Fig. 4b). However, f_{ox} values are higher in the spring and fall sampling times compared to summer for Isunnguata
250 and Russell and approach 50% in the spring, while Kiattut Sermiat values decrease throughout the melt season.

CH_4 concentrations are unrelated to Watson River average daily discharge for Isunnguata, but significantly negatively correlated for Russell (Fig. 5a). The fraction of CH_4 oxidized is moderately negatively correlated with discharge for both Isunnguata and Russell, though the relationship is not significant for either site (Fig. 5b). Discharge is positively correlated with ε_c for both Isunnguata and Russell (Fig. 5c). While the relationship is only significant for Isunnguata, the slopes and
255 intercepts of regression lines for Isunnguata and Russell are similar.

3.3 Mineral weathering and CO_2 models

Mineral weathering leads to net sequestration of CO_2 at all three sites (Fig. 6a). The magnitude of Net ΔCO_2 differs between sites with average values lowest at Isunnguata (-39±37 µM) followed by Russell (-65±32 µM) and Kiattut Sermiat (-98±17 µM). Individual mineral weathering reactions produce differing contributions between sites and over the melt season,
260 with notable differences between Watson River sites (Isunnguata and Russell) and Kiattut Sermiat (Fig. 6b). For instance, the proportional contribution of $Carb_{SA}$ is similar between Isunnguata (17±11%) and Russell (15±6%), though is lower at Kiattut Sermiat (8±1%; Fig. 6b). Kiattut Sermiat has a relatively greater contribution from $Carb_{CA}$ (62±2%) compared to Isunnguata (41±10%) and Russell (38±6%), while Sil_{CA} is lower at Kiattut Sermiat (28±1%) compared to Isunnguata (41±17%), and Russell (47±11%). Kiattut Sermiat additionally exhibits low seasonal variability in the proportional contributions of individual
265 mineral weathering reactions compared to Isunnguata and Russell sites.

$CO_{2\text{-total}}$ represents CO_2 concentrations in the subglacial environment prior to addition and/or consumption of CO_2 through mineral weathering (Eq. 10; Fig. 7). Because the Net $CO_{2\text{-MW}}$ is always negative (more consumption then production), the value of $CO_{2\text{-total}}$ is always greater than measured concentrations ($CO_{2\text{-measured}}$). Regardless of differences in $CO_{2\text{-measured}}$ between sites, the average $CO_{2\text{-total}}$ values are similar between sites and average 91±47 µM for Isunnguata, 94±33 µM for
270 Russell, and 117±16 µM for Kiattut Sermiat.

Keeling plots between $[CO_{2\text{-total}}]^{-1}$ and $\delta^{13}C\text{-}CO_2$ indicate no linear relationship for Russell or Kiattut Sermiat samples, however a strong linear correlation is observed for Isunnguata (r^2=0.99; $p<0.001$) with the removal of one outlier, which also had the lowest $CO_{2\text{-total}}$ value (Fig 8a). Isunnguata samples also show a significant positive correlation between the magnitude of $CO_{2\text{-total}}$ and NH_4 concentrations (r^2=0.73; $p<0.05$), unlike Russell or Kiattut Sermiat samples, though several Russell
275 samples fall close to the regression line between $CO_{2\text{-total}}$ and NH_4 of Isunnguata samples (Fig. 8b).

https://doi.org/10.5194/tc-2020-155
Preprint. Discussion started: 3 July 2020

Because Isunnguata samples exhibit a linear relationship between $[CO_{2\text{-total}}]^{-1}$ and $\delta^{13}C\text{-}CO_2$ consistent with two endmember mixing, we utilize the $\delta^{13}C\text{-}CO_2$ of samples and end members defined by the Keeling plot in an isotopic mixing model to calculate the relative contributions of CO_2 sources to $CO_{2\text{-total}}$. We take the y-intercept (-27.5‰; Fig. 8a) of the Keeling plot regression as the $\delta^{13}C\text{-}CO_2$ for the high-CO_2 end member (assumed to be generated by OM remineralization; $CO_{2\text{-OM}}$) and assume atmospheric CO_2 as the low-CO_2 end member ($CO_{2\text{-atm}}$; $\delta^{13}C\text{-}CO_2$ = -8‰). The relative ($\%CO_{2\text{-atm}}$ and $\%CO_{2\text{-OM}}$) and absolute ($CO_{2\text{-atm}}$ and $CO_{2\text{-OM}}$) contributions of these CO_2 sources to Isunnguata $CO_{2\text{-total}}$ vary throughout the melt season, with $CO_{2\text{-OM}}$ being the dominant source in the early and late melt season while $CO_{2\text{-atm}}$ is the dominant source in the mid-melt season (Fig. 9a). The absolute magnitude of $CO_{2\text{-OM}}$ is approximately 5-10 times greater in the early (89 µM) and late (117 µM) melt seasons compared to mid-melt seasons (13-23 µM), while the magnitude of $CO_{2\text{-atm}}$ varies relatively little throughout the melt season at around 50 µM (Fig. 9b). Both $\%CO_{2\text{-atm}}$ and $\%CO_{2\text{-OM}}$ are significantly ($p<0.05$) correlated with Watson River discharge, and the correlation is positive for $\%CO_{2\text{-atm}}$ and negative for $\%CO_{2\text{-OM}}$ (Fig. 9c). The magnitude of $CO_{2\text{-OM}}$ exhibits a power-law relationship with discharge and is highest at lowest discharge, while the magnitude of $CO_{2\text{-atm}}$ is invariable as a function of discharge (Fig. 9d).

4 Discussion

We observe orders of magnitude variability in dissolved CH_4 and CO_2 concentrations in subglacial discharge of the GrIS, indicating significant differences in the magnitudes of the sources and sinks of these gases across time and space. Supersaturation of both CO_2 and CH_4 with respect to atmospheric concentrations indicates that Isunnguata discharge is a source of both gases to the atmosphere, neighboring Russell Glacier discharges water that is a source of CH_4 but near equilibrium with respect to CO_2, while Kiattut Sermiat in southern Greenland is a sink of atmospheric CO_2 but near equilibrium with respect to CH_4 (Fig. 3e, g). Because CH_4 dynamics may be largely microbially driven while CO_2 dynamics include microbial as well as abiotic mineral weathering processes, we first discuss CH_4 dynamics including a comparison of concentrations, isotopic compositions, and extent of oxidation between sites and over the melt season. We then discuss CO_2 concentrations, impacts of mineral weathering reactions (Table 1), and an assessment of subglacial CO_2 sources, including OM remineralization. These assessments will contribute to our understanding of the variability and controls of CH_4 and CO_2 concentrations in subglacial discharge from the GrIS and may improve predictions of the impact of future ice melt on Arctic carbon budgets.

4.1 Sources and sinks of CH_4

Differences in CH_4 concentrations and relationships with discharge between sites imply heterogeneity in both the extent and controls of subglacial methanogenesis under the GrIS. CH_4 supersaturation occurs at the two subglacial discharge sites that flow to the Watson River (Isunnguata and Russell), and concentrations are similar to the ranges reported in discharge of the Leverett Glacier (up to 600 nM; Lamarche-Gagnon et al., 2019), adjacent to the Russell Glacier in this study. However,

https://doi.org/10.5194/tc-2020-155
Preprint. Discussion started: 3 July 2020

CH_4 concentrations are near atmospheric equilibrium for the Kiattut Sermiat site (Fig 2e). Because methanogenesis is an anaerobic OM remineralization pathway, it is more likely to occur in subglacial environments isolated from atmospheric O_2 sources. Widespread observations of methanogenesis in glacial meltwater of southwest Greenland from this and other studies (Christiansen and Jørgensen, 2018; Dieser et al., 2014; Lamarche-Gagnon et al., 2019), and limited observations of CH_4 in subglacial discharge in southern Greenland, suggests heterogeneity in subglacial conditions that support methanogenesis. This heterogeneity may include variations in the distribution of subglacial organic substrates, such as subglacial permafrost reservoirs identified in previous studies (Ruskeeniemi et al., 2018), which were implicated as an OM source to drive methanogenesis under the Leverett Glacier (Lamarche-Gagnon et al., 2019). Organic deposits under the GrIS may have formed as a consequence of Holocene ice margin fluctuations following the encroachment of ice over previously established soils and terrestrial vegetation (Ruskeeniemi et al., 2018). Methanogenesis fueled by organic material overridden during ice sheet growth has been suggested as a potential climate feedback over glacial interglacial timescales (Wadham et al., 2008), and may contribute to variations in CH_4 concentrations between southwest and southern sites in this study.

Subglacial methanogenesis may additionally be controlled by hydrologic factors as the subglacial hydrological network develops throughout the melt season and channelization of meltwater conduits increases subglacial drainage efficiency (Andrews et al., 2015; Cowton et al., 2013). Drainage efficiency impacts both subglacial water residence time as well the transport of aerobic supraglacial meltwater to the ice bed. Both residence time and oxygen delivery may impact subglacial redox status and methanogenesis potential, and favor methanogenesis when oxygen supply rates are low compared to OM remineralization rates. This condition is most likely to be met in distributed subglacial systems that are hydrologically isolated with limited inputs from aerobic supraglacial meltwater. Such a hydrologic control on methanogenesis at the Russell Glacier is supported by the significant negative correlation between CH_4 concentrations and Watson River average daily discharge (Fig. 5a), suggesting that CH_4 production occurs predominantly during periods of low discharge and greater residence time. Alternatively, higher CH_4 concentrations during low discharge could result from the dilution of relatively small volumes of methanogenic subglacial meltwater with increasing volumes of aerobic supraglacial meltwater. The lack of relationship between CH_4 concentrations and discharge at the Isunnguata Glacier may indicate a greater influence of subglacial outburst events, in which hydrologically isolated methanogenic meltwater pockets are stochastically drained as the subglacial drainage network extends throughout the melt season (Fig. 5a). Subglacial outburst events were also implicated by heterogeneous CH_4 concentrations in subglacial discharge of the Leverett Glacier, and could contribute to heterogeneity in CH_4 concentrations at the Isunnguata Glacier (Lamarche-Gagnon et al., 2019).

While our results suggest heterogeneity in the extent and controls of methanogenesis between outlet glaciers, the microbial methanogenesis pathway as well as CH_4 oxidation dynamics are consistent between sites. Methanogenesis pathways may be evaluated by $\delta^{13}C\text{-}CH_4$ as well as ε_c values because methanogenesis pathways impart different isotopic signatures to CH_4 and CO_2 (Whiticar and Schoell, 1986). Dieser et al. (2014) measured a microbial $\delta^{13}C\text{-}CH_4$ production signal at the Russell Glacier with values between -63‰ and -64‰, which was interpreted to reflect a possible combination of CH_4 produced through

https://doi.org/10.5194/tc-2020-155
Preprint. Discussion started: 3 July 2020

both acetoclastic and CO_2 reduction pathways. The most depleted $\delta^{13}C$-CH_4 value measured at the Isunnguata in this study is close to that of Dieser et al. (2014) at -62.7‰ (Fig. 3f), and similar to values reported by Lamarche-Gagnon et al. (2019) for the Leverett Glacier, suggesting similar methanogenesis pathways across this region. While the exact contributions from each methanogenesis pathway cannot be inferred from isotopic information alone, the range of ε_c values at outlet glaciers are consistent with predominantly acetoclastic methanogenesis during the peak melt season (Fig. 4a). However, ε_c values fall below the expected range from acetoclastic methanogenesis during the early and late melt seasons, likely resulting from variations in the extent of subglacial CH_4 oxidation. Seasonal variation in CH_4 oxidation is supported by consistency between ε_c and f_{ox} values, which both indicate the greatest impact of oxidation (approaching 50%) in the early melt season compared to peak melt season (Fig. 4a, b), with additional evidence of elevated CH_4 oxidation in the late melt season at both Isunnguata and Russell glaciers.

The extent of CH_4 oxidation may be controlled by multiple factors including oxygen availability, subglacial residences time, and subglacial hydrology, similar to methanogenesis. A hydrologic control of CH_4 oxidation is supported by relationships between f_{ox} and ε_c with Watson River daily discharge at both Isunnguata and Russell Glaciers: f_{ox} is negatively related with discharge for both sites (Fig. 5b) while ε_c is positively correlated with discharge (Fig. 5c) although the correlation is only significant at Isunnguata. These correlations suggest that CH_4 oxidation is greatest during periods of low flow, which may be associated with greater residence times to allow subglacial CH_4 oxidation. The delivery of oxygen to the subsurface by supraglacial melting does not appear to be a limiting factor in subglacial CH_4 oxidation, which should increase f_{ox} as more oxygenated supraglacial water is delivered to the subglacial system. Instead, the observed greater CH_4 oxidation during periods of low discharge may reflect CH_4 oxidation following mixing between draining methanogenic subglacial meltwater pockets with aerobic subglacial meltwater. Longer transit times during periods of low flow may allow more subglacial methane oxidation to occur than during peak discharge, when the development of channelized flow paths reduces meltwater residence time in the subglacial environment.

Our results indicate a high degree of heterogeneity in subglacial methanogenesis under the GrIS, as well as a significant impact of CH_4 oxidation, which serves to reduce atmospheric CH_4 fluxes. Given the observed heterogeneity in this study, further investigation of the spatial variability in outlet glacier CH_4 concentrations is needed to determine the impact of GrIS loss on Arctic and global CH_4 budgets, while a better understanding of the controls of these differences will improve models of how CH_4 fluxes from subglacial discharge will change with continued warming.

4.2 Sources and sinks of CO_2

Dissolved CO_2 concentrations in subglacial discharge are consistently supersaturated with respect to atmospheric concentrations at Isunnguata Glacier, near atmospheric equilibrium at Russell Glacier, and undersaturated at Kiattut Sermiat Glacier, indicating that glacial meltwater from the GrIS can serve as either a source or sink of CO_2 to the atmosphere. Differences in dissolved CO_2 concentrations also imply variability in carbon processes under the GrIS (Fig. 3g). Because our

https://doi.org/10.5194/tc-2020-155
Preprint. Discussion started: 3 July 2020

approach to assess the magnitude of subglacial CO_2 sources (including subglacial OM remineralization) depends in part on modelling results of CO_2 consumption by mineral weathering (Eq. 10), we first discuss the impacts of mineral weathering reactions, followed by a discussion of subglacial CO_2 sources, including OM remineralization.

4.2.1 Subglacial CO_2 sink: mineral weathering reactions

Although mineral weathering reactions may either increase or decrease dissolved CO_2 concentrations (Table 1), the net impact of mineral weathering at our study sites is to consume CO_2 (Fig. 6a). Net consumption occurs because the CO_2 source from $Carb_{SA}$ is ubiquitously low compared to sinks from either $Carb_{CA}$ or Sil_{CA} (Fig. 6b). The range in Net $CO_{2\text{-}MW}$ is similar between subglacial discharge sites (between 10-150 µM; Fig. 6a), but average values increase from Kiattut Sermiat to Russell to Insunnguata, likely reflecting the relative weatherability of alkaline igneous rocks, granulite facies gneisses, and amphibolite facies gneisses. Kiattut Sermiat is characterized by a relatively high proportion of $Carb_{CA}$ compared to Watson River sites, which may arise from the presence of trace carbonates in abundant readily weatherable basaltic intrusions as has been implicated in other studies (Urra et al., 2019). The relatively greater influence of carbonate dissolution compared to silicate dissolution on Total $CO_{2\text{-}MW}$ at Kiattut Sermiat may also relate to more rapid dissolution kinetics of carbonates, which allow carbonate dissolution to have a large influence on major cation and anion load even when carbonates are only present in trace amounts (Tranter, 2005). At Isunnguata and Russell glaciers, Sil_{CA} has a greater influence than $Carb_{CA}$ on Total $CO_{2\text{-}MW}$, which could result from either a lower abundance of trace carbonates to participate in weathering reactions, or relatively longer subglacial residence times that would allow a greater accumulation of silicate weathering products.

Despite the high impact of $Carb_{CA}$ on Total $CO_{2\text{-}MW}$ at Kiattut Sermiat compared to Isunnguata and Russell sites, $Carb_{SA}$ is notably lower at Kiattut Sermiat than other sites and suggests a limited role for sulfuric acid weathering that may relate to subglacial sulfide oxidation dynamics. Lower abundances of sulfide minerals in the subglacial environment may limit the production of sulfuric acid, and could result from differences in lithology between sites, the depletion of sulfide minerals due to prior weathering (Graly et al., 2014), or weathering occurring in anoxic environments that limit the oxidation of sulfide to sulfuric acid (Deuerling et al., 2019). The kinetics of sulfide oxidation may also significantly differ between sites depending on the relative contributions of abiotic compared to microbially mediated sulfide oxidation, as microbially mediated sulfide oxidation is several orders of magnitude faster than abiotic sulfide oxidation. Rapid microbially mediated sulfide oxidation has been implicated in the development of anaerobic conditions, which could also support subglacial methanogenesis (Sharp et al., 1999). Observations of higher CH_4 concentrations as well as higher contributions of $Carb_{SA}$ at Isunnguata and Russell compared to Kiattut Sermiat in this study may therefore be linked to subglacial microbial activity, which is known to vary based on factors such as the presence of organic and fine-grained rock flour to serve as growth substrates, insulation from fluctuations in temperature, and delivery of nutrients and organic matter from supraglacial sources (Sharp et al., 1999). If microbially driven, our results suggest possible linkages between microbial processes and subglacial mineral weathering regimes, with significant impacts to both CH_4 and CO_2 dynamics due to the role of $Carb_{SA}$ as a CO_2 source (Table 1).

https://doi.org/10.5194/tc-2020-155
Preprint. Discussion started: 3 July 2020

4.2.2 Subglacial CO_2 sources

Mineral weathering leads to net CO_2 consumption in all subglacial discharge samples, and thus the measured CO_2 concentrations represents only a fraction of the total CO_2 that would have been present in the absence of mineral weathering reactions ($CO_{2\text{-total}}$; Eq. 10). CO_2 sources could include dissolution of atmospheric gases in air-filled conduits or fractures in ice, or CO_2 contained in ice bubbles (Fig. 1; Anklin et al., 1995; Graly et al., 2017). CO_2 may also be produced through mechanical grinding and volatilization of fluid inclusions (Macdonald et al., 2018) or OM remineralization. While previous studies have indicated that additional atmospheric CO_2 input through fractures and air-filled conduits may supply sufficient CO_2 to drive the observed extent of mineral weathering in many subglacial environments, including several sites in Greenland (Graly et al., 2017), CH_4 concentrations elevated above atmospheric equilibrium at the two Watson River sites reflects OM remineralization that would also contribute CO_2. While the magnitude of this source and its relative importance compared to other subglacial CO_2 sources is currently unknown, differing sources of carbonic acid for mineral weathering reactions carry different implications for subglacial CO_2 budgets. For instance, carbonic acid weathering driven by invasion of atmospheric CO_2 would represent a sink of atmospheric CO_2, but carbonic acid weathering driven by OM remineralization would instead serve to consume CO_2 from *in situ* sources and limit its potential as an atmospheric source. Determining the sources of carbonic acid to subglacial weathering reactions is therefore critical to understand the controls of mineral weathering in subglacial environments as well as the role of that process in atmospheric CO_2 sequestration.

Comparisons between measured $\delta^{13}C\text{-}CO_2$ in subglacial discharge samples and likely $\delta^{13}C\text{-}CO_2$ values of CO_2 sources indicate that CO_2 sources differ between sites, with OM remineralization as the predominant CO_2 source at the Isunnguata but not at Russell or Kiattut Sermiat glaciers. Keeling plots of $[CO_{2\text{-total}}]^{-1}$ versus $\delta^{13}C\text{-}CO_2$ indicate that $CO_{2\text{-total}}$ at Isunnguata discharge may be represented by a two-end member mixing model, in contrast to Russell and Kiattut Sermiat glaciers (Fig. 8). Mixing model end members include a ^{13}C-enriched, lower-CO_2 source and a ^{13}C-depleted, higher-CO_2 source (Fig. 8a). The y-intercept of the regression between $[CO_{2\text{-total}}]^{-1}$ versus $\delta^{13}C\text{-}CO_2$ (representing the isotopic signature of the high-CO_2 endmember) is -27.4‰, which is close to what would be expected from OM remineralization. For instance, CO_2 from remineralized OM in Greenlandic heath soils ranged between approximately -27 to -25‰ (Ravn et al., 2020), and between -20 to -30‰ for thawed Alaskan permafrost soils (Mauritz et al., 2019), both of which may be similar to subglacial organic matter. An additional correlation is observed between $CO_{2\text{-total}}$ and NH_4 concentrations for Isunnguata samples, which would be expected from OM remineralization (Fig. 8b). The low-CO_2 end member could reflect atmospheric CO_2 input, which should result in a $\delta^{13}C\text{-}CO_2$ value of approximately -8‰. While the $\delta^{13}C\text{-}CO_2$ value of the lowest-$CO_{2\text{-total}}$ samples in the Isunnguata Keeling plot (e.g. highest $[CO_{2\text{-total}}]^{-1}$ not including the outlier) are slightly depleted compared to atmospheric values at -12.1‰ (Fig. 8a), even the lowest CO_2 concentrations measured at Isunnguata are supersaturated with respect to atmospheric concentrations (Fig. 3g). Supersaturation suggests that OM remineralization contributes CO_2 even for low CO_2-concentration samples and isotopically depletes the subglacial CO_2 reservoir.

https://doi.org/10.5194/tc-2020-155
Preprint. Discussion started: 3 July 2020

While both atmospheric CO_2 ($CO_{2\text{-atm}}$) and CO_2 derived from OM remineralization ($CO_{2\text{-OM}}$) provide carbonic acid to drive subglacial mineral weathering as well as CO_2 supersaturation in Isunnguata discharge, their absolute and relative contributions are controlled by different processes. Understanding the controls of CO_2 acquisition may improve understanding of subglacial carbon dynamics as well as the conditions necessary for subglacial environments to become CO_2 sources to the atmosphere. $CO_{2\text{-OM}}$ is the dominant source to $CO_{2\text{-total}}$ at Isunnguata in the early and late melt seasons (Fig. 9a) when discharge is low (Fig. 9c), while $CO_{2\text{-atm}}$ is the dominant CO_2 source in the peak melt season when discharge is high. This switch in dominant CO_2 sources occurs because the magnitude of $CO_{2\text{-OM}}$ has a strong negative association with discharge, approaching zero during maximum discharge times (Fig. 9d), while $CO_{2\text{-atm}}$ remains relatively constant over the melt season (Fig. 9b) and the range of discharges (Fig. 9d). The high contributions of $CO_{2\text{-OM}}$ during low discharge could reflect higher residence times that allow greater biogeochemical modification and accumulation of OM remineralization reaction products, including CO_2. The chemostatic behavior for $CO_{2\text{-atm}}$ indicates that invasion of atmospheric CO_2 is independent of the extent of chemical weathering, which exhibits strong seasonal variation (Fig. 6a). Chemostatic behavior of $CO_{2\text{-atm}}$ may indicate that $CO_{2\text{-OM}}$ maintains CO_2 concentrations at or above atmospheric saturation concentrations, and no additional atmospheric CO_2 dissolution would be needed to maintain equilibrium. Chemostatic behavior of $CO_{2\text{-atm}}$ could additionally indicate that the Isunnguata subglacial drainage is largely closed to atmospheric exchange. Both mechanisms are supported by the consistent CO_2 supersaturation observed in subglacial discharge at Isunnguata (Fig. 3g), which suggests that limited atmospheric exchange prevents significant outgassing prior to discharge. These results first imply that CO_2 supersaturation due to OM remineralization is likely during low flow conditions in systems that are relatively closed to the atmosphere. Moreover, $CO_{2\text{-OM}}$ is the main driver for mineral weathering during low-flow conditions: while $CO_{2\text{-MW}}$ exceeds -150 µM late in the melt season (Fig. 6a), $CO_{2\text{-atm}}$ provides only about a third of this CO_2 (Fig.8b), suggesting that the remainder was driven by $CO_{2\text{-OM}}$. In this case, only a fraction of the mineral weathering products measured in subglacial outflow at Isunnguata are directly involved in the sequestration of atmospheric CO_2, and the majority of mineral weathering serves to consume CO_2 from *in situ* $CO_{2\text{-OM}}$ production.

While $\delta^{13}C\text{-}CO_2$ values of Russell and Kiattut Sermiat samples are within the range of Isunnguata samples, suggesting possible contributions of $CO_{2\text{-atm}}$ and $CO_{2\text{-OM}}$, non-linear Keeling plots indicate variability in the CO_2 concentration and/or isotopic composition of end members, or significant contributions of at least one other major subglacial CO_2 source. We address both possibilities here. While atmospheric CO_2 should be relatively invariable, $CO_{2\text{-OM}}$ may vary both in concentration and isotopic composition, depending on variability in the quantity and composition of organic deposits, as well as remineralization rates. For instance, if remineralization largely occurs in hydrologically isolated subglacial meltwater pockets, some variability in the concentration and $\delta^{13}C\text{-}CO_2$ of $CO_{2\text{-OM}}$ is likely. While no data yet exist to characterize the variability in subglacial OM reservoirs, variability in either concentration or isotopic composition of $CO_{2\text{-OM}}$ could plausibly result in non-linear Keeling plots here.

https://doi.org/10.5194/tc-2020-155
Preprint. Discussion started: 3 July 2020

Additional subglacial CO_2 sources could include atmospheric CO_2 contained in ice bubbles, or lithogenic CO_2 liberated by mechanical grinding, though both of these sources would be expected to enrich rather than deplete the $\delta^{13}C$-CO_2 values of the samples relative to modern atmospheric $\delta^{13}C$-CO_2 values. Ice bubbles contain gaseous CO_2 at concentrations and isotopic compositions reflecting atmospheric conditions during ice formation. While heterogeneity may result from gas bubbles recording changes in atmospheric CO_2, variability in $\delta^{13}C$-CO_2 of gas bubble CO_2 should be only a few per mil, which is small compared to the variation observed in Russell and Kiattut Sermiat samples (Tipple et al., 2010; Fig. 8a). Gas bubble CO_2 should also be ^{13}C-enriched compared to modern atmospheric CO_2 due to fossil fuel contributions, and thus would be unlikely to cause the variation in sample $\delta^{13}C$-CO_2 values that are more ^{13}C-depleted than modern atmospheric $\delta^{13}C$-CO_2 values (Fig. 8a). Recent work has also highlighted the potential for subglacial mechanical grinding to result in CO_2 production through the volatilization of fluid inclusions (Macdonald et al., 2018). While volatilization of fluid inclusions through mechanical grinding was found to produce sufficient CO_2 to drive approximately 20% of mineral weathering in Svalbard subglacial environments, the expected isotopic composition of lithogenic CO_2 is more ^{13}C-enriched than our measured $\delta^{13}C$-CO_2 values. Because mechanical grinding should produce CO_2 with an isotopic composition reflecting the lithogenic source, (Lüders et al., 2012), its contributions here are likely limited. For instance, estimates of $\delta^{13}C$ for bulk hydrocarbons in fluid inclusions in the Ilímaussaq alkaline complex of South Greenland have values of -4.5±1.5‰ (Madsen, 2001), which is close to the $\delta^{13}C$-CO_2 of CO_2 in fluid inclusions in the Bamble granulite sector of South Norway (~ -6‰; Newton et al., 1980). There is an additional possibility of atmospheric exchange between the subglacial outlet site and our water sampling sites that could serve as an additional CO_2 source or sink. However, atmospheric CO_2 exchange after discharge would have the same impact on Keeling plots as atmospheric CO_2 exchange prior to discharge. Although Kiattut Sermiat CO_2 concentrations are undersaturated with respect to atmospheric concentrations and would promote invasion of atmospheric CO_2, measured $\delta^{13}C$-CO_2 values are more ^{13}C-depleted than modern atmospheric CO_2 and are not consistent with atmospheric CO_2 as the sole or dominant source of CO_2 to glacial meltwater samples (Fig. 8a). While more information is needed to determine the sources of CO_2 to Russell and Kiattut Sermiat samples, $\delta^{13}C$-CO_2 values of samples from both sites imply mixing between a ^{13}C-depleted CO_2 source, such as OM remineralization, and one or more ^{13}C-enriched CO_2 sources, such as atmospheric or lithogenic CO_2.

5 Conclusions

Subglacial reactions impact the concentrations of CO_2 and CH_4 in subglacial discharge of GrIS, which act as either sources or sinks of GHG to the atmosphere. CH_4 concentrations of subglacial discharge are likely controlled by the availability of subglacial OM to drive methanogenesis as well as the extent of CH_4 oxidation. Regional differences in subglacial OM deposits may account for the occurrence of methanogenesis in southwest outlet glaciers (Isunnguata and Russell) in this and other studies, contrasting with southern Kiattut Sermiat where little CH_4 production occurs. During the early melt season, oxidation consumes nearly 50% of CH_4 produced at southwest sites, and relationships between discharge and CH_4 oxidation

https://doi.org/10.5194/tc-2020-155
Preprint. Discussion started: 3 July 2020

(ε_c and f_{ox}) suggest that CH_4 oxidation depends on longer subglacial residence time during periods of low discharge. While mineral weathering consumes CO_2 throughout the melt season at all three sites, additional CO_2 resupplied from atmospheric and subglacial sources increases the CO_2 concentrations of subglacial discharge. The magnitude of additional CO_2 sources ($CO_{2\text{-total}}$) is insufficient to maintain atmospheric equilibrium at Kiattut Sermiat, leading subglacial discharge to be a sink of atmospheric CO_2, while $CO_{2\text{-total}}$ maintains close to atmospheric equilibrium concentrations at the Russell Glacier. At Isunnguata, however, OM remineralization produces more CO_2 than is consumed by mineral weathering and causes meltwater to be a source of CO_2 to the atmosphere. This finding implies that subglacial mineral weathering serves to partially or fully consume CO_2 produced from *in situ* sources under the GrIS but does not necessarily result in direct consumption of modern atmospheric CO_2. The important role of OM remineralization in subglacial environments of the GrIS determined by this and other studies also implies links between subglacial OM deposits and export of other biogeochemical solutes from the GrIS, including nutrients as well as redox-sensitive elements. While the export of nutrients from the GrIS has been the focus of numerous studies (Bhatia et al., 2013; Hawkings et al., 2016; Lawson et al., 2014), little is currently known regarding the role of OM sources in governing these exports. Given the variability in GHG concentrations observed in this study, constraining the extent of heterogeneity in outlet glaciers of the GrIS as well as the biogeochemical, hydrologic, and geologic controls of this heterogeneity will be important for upscaling atmospheric fluxes as well as efforts to predict impacts of ice loss on carbon budgets due to current and future melting of the GrIS.

Author Contribution

Jonathan B. Martin and Ellen E. Martin participated in conceptualization, data collection, data interpretation, reviewing and editing the manuscript, and acquired the funding for this project. Shaily Rahman participated in data collection and early interpretation and presentation of results. Andrea J. Pain participated in conceptualization, data collection, analysis, and interpretation, and took the lead on writing the manuscript with contributions from Jonathan B. Martin and Ellen E. Martin.

Acknowledgements

We acknowledge the members of our field teams: Daniel Fischer, Fabio Da Prat, Hailey Hall, Mark Robbins, and Scott Schnur. Additional invaluable support was provided by Steven DiEgidio, Nini Frydkjær Brandt, Inga Gisladottir, and Jacky Simoud. We are grateful for the excellent field support provided by the Kangerlussuaq International Science Station and Polar Field Services (CH2M Hill). This work was funded by the National Science Foundation grant (ANS-1603452). Discharge data from Watson River were gathered by B. Hasholt and A.B. Mikkelsen on behalf of the University of Copenhagen (2006-2013), and by D. van As and B. Hasholt on behalf of the Geological Survey of Denmark and Greenland (2014-present). The authors declare that they have no conflict of interest. Data is accessible on the Arctic Data Center (doi:10.18739/A2F76672G) including gas and nutrient data (https://cn.dataone.org/cn/v2/resolve/urn:uuid:c1051a07-cbdf-4061-ae44-c1472f61e3fe) and major

https://doi.org/10.5194/tc-2020-155
Preprint. Discussion started: 3 July 2020

element concentrations used for geochemical modeling (https://cn.dataone.org/cn/v2/resolve/urn:uuid:65d272f6-d280-4fcc-8aaa-4805f12ca6ae).

References

Andrews, L. C., Catania, G. A., Hoffman, M. J., Gulley, J. D., Lüthi, M. P., Ryser, C., Hawley, R. L. and Neumann, T. A.: Direct observations of evolving subglacial drainage beneath the Greenland Ice Sheet, Nature, 514(7520), 80–83, doi:10.1038/nature13796, 2015.

Anklin, M., Barnola, J. M. M., Schwander, J., Stauffer, B. and Raynaud, D.: Processes affecting the CO2 concentrations measured in Greenland ice, Tellus B, 47(4), 461–470, doi:10.1034/j.1600-0889.47.issue4.6.x, 1995.

van As, D., Hasholt, B., Ahlstrøm, A. P., Box, J. E., Cappelen, J., Colgan, W., Fausto, R. S., Mernild, S. H., Bech, A., Noël, B. P. Y., Petersen, D. and van Den Broeke, M. R.: Reconstructing Greenland Ice Sheet meltwater discharge through the Watson River (1949–2017), Arctic, Antarct. Alp. Res., 50(1), doi:10.1080/15230430.2018.1433799, 2018.

van As, D., Mikkelsen, A. B., Nielsen, M. H., Box, J. E., Liljedahl, L. C., Lindbäck, K., Pitcher, L. and Hasholt, B.: Hypsometric amplification and routing moderation of Greenland ice sheet meltwater release, Cryosphere, 11(3), 1371–1386, doi:10.5194/tc-11-1371-2017, 2017.

van As, D., Hasholt, B., Ahlstrøm, A. P., Box, J. E., Cappelen, J., Colgan, W., Fausto, R. S., Mernild, S. H., Bech, A., Noël, B. P. Y., Petersen, D., Broeke, M. R. Van Den, As, D. Van, Hasholt, B., Ahlstrøm, A. P., Box, J. E., Colgan, W., Fausto, R. S., Mernild, S. H. and Mikkelsen, A. B.: Reconstructing Greenland Ice Sheet meltwater discharge through the Watson River (1949 – 2017) Reconstructing Greenland Ice Sheet meltwater discharge through the Watson, Arctic, Antarct. Alp. Res., 50(1), doi:10.1080/15230430.2018.1433799, 2018.

Berner, R. A., Lasaga, A. C. and Garrels, R. M.: The carbonate-silicate geochemical cycle and its effect on atmospheric carbon dioxide over the past 100 million years., Am. J. Sci., 283(7), 641–683, doi:10.2475/ajs.283.7.641, 1983.

Bhatia, M. P., Kujawinski, E. B., Das, S. B., Breier, C. F., Henderson, P. B. and Charette, M. A.: Greenland meltwater as a significant and potentially bioavailable source of iron to the ocean, Nat. Geosci., 6(4), 274–278, doi:10.1038/ngeo1746, 2013.

Christiansen, J. R. and Jørgensen, C. J.: First observation of direct methane emission to the atmosphere from the subglacial domain of the Greenland Ice Sheet, Sci. Rep., 8(1), 2–7, doi:10.1038/s41598-018-35054-7, 2018.

Cowton, T., Nienow, P., Sole, A., Wadham, J., Lis, G., Bartholomew, I., Mair, D. and Chandler, D.: Evolution of drainage system morphology at a land - terminating Greenlandic outlet glacier, , 118, 29–41, doi:10.1029/2012JF002540, 2013.

Deuerling, K. M., Martin, J. B., Martin, E. E. and Scribner, C. A.: Hydrologic exchange and chemical weathering in a proglacial watershed near Kangerlussuaq, west Greenland, J. Hydrol., 556, 220–232, doi:10.1016/j.jhydrol.2017.11.002, 2018.

https://doi.org/10.5194/tc-2020-155
Preprint. Discussion started: 3 July 2020

Deuerling, K. M., Martin, J. B., Martin, E. E., Abermann, J., Myreng, S. M., Petersen, D. and Rennermalm, A. K.: Chemical weathering across the western foreland of the Greenland Ice Sheet, Geochim. Cosmochim. Acta, 245(245), 426–440, doi:10.1016/j.gca.2018.11.025, 2019.

Dieser, M., Broemsen, E. L. J. E., Cameron, K. A., King, G. M., Achberger, A., Choquette, K., Hagedorn, B., Sletten, R., Junge, K. and Christner, B. C.: Molecular and biogeochemical evidence for methane cycling beneath the western margin of the Greenland Ice Sheet, ISME J., 8(11), 2305–2316, doi:10.1038/ismej.2014.59, 2014.

van Gool, J. A., Alsop, G. I., Arting, U. E., Garde, A. A., Knudsen, C., Krawiec, A. W., Mazur, S., Nygaard, J., Piazolo, S. and Thomas, C. W.: Precambrian geology of the northern Nagssugtoqidian orogen, West Greenland: mapping in the Kangaatsiaq area, Geol. Greenl. Surv. Bull., 191, 13–23, 2002.

Graly, J., Harrington, J. and Humphrey, N.: Combined diurnal variations of discharge and hydrochemistry of the Isunnguata Sermia outlet, Greenland Ice Sheet, Cryosphere, 11(3), 1131–1140, doi:10.5194/tc-11-1131-2017, 2017a.

Graly, J. A., Humphrey, N. F., Landowski, C. M. and Harper, J. T.: Chemical weathering under the Greenland Ice Sheet, Geology, 551–554, doi:10.1130/G35370.1, 2014.

Graly, J. A., Drever, J. I. and Humphrey, N. F.: Calculating the balance between atmospheric CO2 drawdown and organic carbon oxidation in subglacial hydrochemical systems, Global Biogeochem. Cycles, 31(4), 709–727, doi:10.1002/2016GB005425, 2017b.

Hasholt, B., As, D. Van, Mikkelsen, A. B., Mernild, S. H., Yde, J. C., Hasholt, B., As, D. Van, Mikkelsen, A. B., Mernild, S. H. and Hasholt, B.: Observed sediment and solute transport from the Kangerlussuaq sector of the Greenland Ice Sheet (2006 – 2016), Arctic, Antarct. Alp. Res., 50(1), doi:10.1080/15230430.2018.1433789, 2018.

Hawkings, J., Wadham, J., Tranter, M., Telling, J. and Bagshaw, E.: The Greenland Ice Sheet as a hot spot of phosphorus weathering and export in the Arctic, Global Biogeochem. Cycles, 191–210, doi:10.1002/2015GB005237.Received, 2016.

Henriksen, N., Higgins, A. K., Kalsbeek, F. and Pulvertaft, T. C. R.: Greenland from Archaean to Quaternary. Descriptive text to the 1995 Geological map of Greenland, 1:2 500 000. 2nd edition, GEUS Bull., 18(SE-MONOGRAPH), 1–126, doi:10.34194/geusb.v18.4993, 2009.

Hindshaw, R. S., Rickli, J., Leuthold, J., Wadham, J. and Bourdon, B.: Identifying weathering sources and processes in an outlet glacier of the Greenland Ice Sheet using Ca and Sr isotope ratios, Geochim. Cosmochim. Acta, 145, 50–71, doi:10.1016/j.gca.2014.09.016, 2014.

Kalsbeek, F. and Taylor, P. N.: Isotopic and chemical variation in granites across a Proterozoic continental margin- the Ketilidian mobile belt of South Greenland, 1Earth Planet. Sci. Lett., 73(1), 65–80, 1985.

Keeling, C. D.: The concentration and isotopic abundances of atmospheric carbon dioxide in rural areas, Geochim.

Cosmochim. Acta, 13(4), 322–334, doi:10.1016/0016-7037(58)90033-4, 1958.

Lamarche-Gagnon, G., Wadham, J. ., Sherwood Lollar, B., Arndt, S., Fietzek, P., Beaton, A. D., Tedstone, A. J., Telling, J., Bagshaw, E. A., Hawkings, J. R., Kohler, T. J., Zarsky, J. D., Mowlem, M. C., Anesio, A. M. and Stibal, M.: Greenland melt drives continuous export of methane from the ice-sheet bed, Nature, 565(7737), 73–77, doi:http://dx.doi.org/10.1038/s41586-018-0800-0, 2019.

Larsen, N. K., Find, J., Kristensen, A., Bjørk, A. A., Kjeldsen, K. K., Odgaard, B. V, Olsen, J. and Kjær, K. H.: Holocene ice marginal fluctuations of the Qassimiut lobe in South Greenland, Nat. Publ. Gr., 1–11, doi:10.1038/srep22362, 2016.

Lawson, E. C., Wadham, J. L., Tranter, M., Stibal, M., Lis, G. P., Butler, C. E. H., Laybourn-Parry, J., Nienow, P., Chandler, D. and Dewsbury, P.: Greenland ice sheet exports labile organic carbon to the arctic oceans, Biogeosciences, 11(14), 4015–4028, doi:10.5194/bg-11-4015-2014, 2014.

Lindbäck, K., Pettersson, R., Hubbard, A. L., Doyle, S. H., As, D., Mikkelsen, A. B. and Fitzpatrick, A. A.: Subglacial water drainage, storage, and piracy beneath the Greenland ice sheet, , 7606–7614, doi:10.1002/2015GL065393.Received, 2015.

Lüders, V., Plessen, B. and di Primio, R.: Stable carbon isotopic ratios of CH 4-CO 2-bearing fluid inclusions in fracture-fill mineralization from the Lower Saxony Basin (Germany) - A tool for tracing gas sources and maturity, Mar. Pet. Geol., 30(1), 174–183, doi:10.1016/j.marpetgeo.2011.10.006, 2012.

Ludwig, W., Amiotte Suchet, P. and Probst, J.-L.: Enhanced chemical weathering of rocks during the last glacial maximum: a sink for atmospheric CO2?, Chem. Geol., 159, 147–161, 1999.

Macdonald, M. L., Wadham, J. L., Telling, J. and Skidmore, M. L.: Glacial Erosion Liberates Lithologic Energy Sources for Microbes and Acidity for Chemical Weathering Beneath Glaciers and Ice Sheets, Front. Earth Sci., 6(November), 1–15, doi:10.3389/feart.2018.00212, 2018.

Madsen, J. K.: A review of the composition and evolution of hydrocarbon gases during solidification of the Ilímaussaq alkaline complex, South Greenland, Geol. Greenl. Surv. Bull., 190, 159–166, 2001.

Mahieu, K., De Visscher, A., Vanrolleghem, P. A. and Van Cleemput, O.: Modelling of stable isotope fractionation by methane oxidation and diffusion in landfill cover soils, Waste Manag., 28(9), 1535–1542, doi:10.1016/j.wasman.2007.06.003, 2008.

Mauritz, M., Celis, G., Ebert, C., Hutchings, J., Ledman, J., Natali, S. M., Pegoraro, E., Salmon, V. G., Schädel, C., Taylor, M. and Schuur, E. A. G.: Using Stable Carbon Isotopes of Seasonal Ecosystem Respiration to Determine Permafrost Carbon Loss, J. Geophys. Res. Biogeosciences, 124(1), 46–60, doi:10.1029/2018JG004619, 2019.

Mouginot, J., Rignot, E., Bjørk, A. A., van den Broeke, M., Millan, R., Morlighem, M., Noël, B., Scheuchl, B. and Wood, M.: Forty-six years of Greenland Ice Sheet mass balance from 1972 to 2018, Proc. Natl. Acad. Sci., 116(19), 201904242, doi:10.1073/pnas.1904242116, 2019.

https://doi.org/10.5194/tc-2020-155
Preprint. Discussion started: 3 July 2020

Musilova, M., Tranter, M., Wadham, J., Telling, J., Tedstone, A. and Anesio, A. M.: Microbially driven export of labile organic carbon from the Greenland ice sheet, Nat. Geosci., 10(5), 360–365, doi:10.1038/ngeo2920, 2017.

Myrttinen, A., Becker, V. and Barth, J. A. C.: A review of methods used for equilibrium isotope fractionation investigations between dissolved inorganic carbon and CO 2, Earth-Science Rev., 115(3), 192–199, doi:10.1016/j.earscirev.2012.08.004, 2012.

Newton, R. C., Smith, J. V. and Windley, B. F.: Carbonic metamorphism, granulites and crustal growth, Nature, 288(5786), 45–50, doi:10.1038/288045a0, 1980.

Pain, A. J., Martin, J. B. and Young, C. R.: Sources and sinks of CO2 and CH4 in siliciclastic subterranean estuaries, Limnol. Oceanogr., 64(4), 1500–1514, doi:10.1002/lno.11131, 2019.

Parkhurst, L.: Geochemical mole-balance modeling with uncertain data, Water Resour. Res., 33(8), 1957–1970, 1997.

St. Pierre, K. A., St. Louis, V. L., Schiff, S. L., Lehnherr, I., Dainard, P. G., Gardner, A. S., Aukes, P. J. K. and Sharp, M. J.: Proglacial freshwaters are significant and previously unrecognized sinks of atmospheric CO 2, Proc. Natl. Acad. Sci., 116(36), 17690–17695, doi:10.1073/pnas.1904241116, 2019.

Da Prat, F. A. and Martin, E.: Weathering in the Glacial Foreland of Southern and Western Greenland, Univ. Florida J. Undergrad. Res., 20(2), doi:10.32473/ufjur.v20i2.106168, 2019.

Preuss, I., Knoblauch, C., Gebert, J. and Pfeiffer, E. M.: Improved quantification of microbial CH4 oxidation efficiency in arctic wetland soils using carbon isotope fractionation, Biogeosciences, 10(4), 2539–2552, doi:10.5194/bg-10-2539-2013, 2013.

Ravn, N. R., Elberling, B. and Michelsen, A.: Arctic soil carbon turnover controlled by experimental snow addition, summer warming and shrub removal, Soil Biol. Biochem., 142(December 2019), 107698, doi:10.1016/j.soilbio.2019.107698, 2020.

Rennermalm, A. K., Smith, L. C., Chu, V. W., Forster, R. R., Box, J. E. and Hagedorn, B.: Proglacial river stage, discharge, and temperature datasets from the Akuliarusiarsuup Kuua River northern tributary, Southwest Greenland, 2008–2011, Earth Syst. Sci. Data Discuss., 2100(4), 1–12, doi:10.5194/essd-4-1-2012, 2012.

Rennermalm, A. K., Smith, L. C., Chu, V. W., Box, J. E., Forster, R. R., Broeke, M. R. Van Den and As, D. Van: Evidence of meltwater retention within the Greenland ice sheet, Cryosph., 1433–1445, doi:10.5194/tc-7-1433-2013, 2013.

Repo, M. E., Huttunen, J. T., Naumov, A. V., Chichulin, A. V., Lapshina, E. D., Bleuten, W. and Martikainen, P. J.: Release of CO2 and CH4 from small wetland lakes in western Siberia, Tellus, Ser. B Chem. Phys. Meteorol., 59(5), 788–796, doi:10.1111/j.1600-0889.2007.00301.x, 2007.

Ruskeeniemi, T., Engström, J., Lehtimäki, J., Vanhala, H., Korhonen, K., Kontula, A., Claesson Liljedahl, L., Näslund, J. O. and Pettersson, R.: Subglacial permafrost evidencing re-advance of the Greenland Ice Sheet over frozen ground, Quat. Sci.

Rev., 199, 174–187, doi:10.1016/j.quascirev.2018.09.002, 2018.

Ryu, J. S. and Jacobson, A. D.: CO2 evasion from the Greenland Ice Sheet: A new carbon-climate feedback, Chem. Geol., 320–321, 80–95, doi:10.1016/j.chemgeo.2012.05.024, 2012.

Sharp, M., Parkes, J., Cragg, B., Fairchild, I. J., Lamb, H. and Tranter, M.: Widespread bacterial populations at glacier beds and their relationship to rock weathering and carbon cycling, Geology, 27(2), 107–110, doi:10.1130/0091-7613(1999)027<0107:WBPAGB>2.3.CO;2, 1999.

Tipple, B. J., Meyers, S. R. and Pagani, M.: Carbon isotope ratio of Cenozoic CO 2 : A comparative evaluation of available geochemical proxies , Paleoceanography, 25(3), 1–11, doi:10.1029/2009pa001851, 2010.

Tranter, M.: Geochemical Weathering in Glacial and Proglacial Environments, in Surface and Ground Water, Weathering, and Soils : Treatise on Geochemistry, vol. 5, edited by J. I. Drever., 2005.

Upton, B. G. J., Emeleus, C. H., Heaman, L. M., Goodenough, K. M. and Finch, A. A.: Magmatism of the mid-Proterozoic Gardar Province, South Greenland: Chronology, petrogenesis and geological setting, Lithos, 68(1–2), 43–65, doi:10.1016/S0024-4937(03)00030-6, 2003.

Urra, A., Wadham, J., Hawkings, J. R., Telling, J., Hatton, J. E., Yde, J. C., Hasholt, B., van As, D., Bhatia, M. P. and Nienow, P.: Weathering Dynamics Under Contrasting Greenland Ice Sheet Catchments, Front. Earth Sci., 7(November), doi:10.3389/feart.2019.00299, 2019.

de Visscher, A., de Pourcq, I. and Chanton, J.: Isotope fractionation effects by diffusion and methane oxidation in landfill cover soils, J. Geophys. Res. Atmos., 109(18), 1–8, doi:10.1029/2004JD004857, 2004.

Wadham, J. L., Tranter, M., Tulaczyk, S. and Sharp, M.: Subglacial methanogenesis : A potential climatic amplifier ?, Global Biogeochem. Cycles, 22(December 2007), 1–16, doi:10.1029/2007GB002951, 2008.

Walker, J. C. G., Hays, P. B. and Kasting, J. F.: A negative feedback mechanism for the long-term stabilization of earth's surface temperature, J. Geophys. Res., 86(1), 9776–9782, 1981.

Warren, C. R. and Glasser, N. F.: Contrasting response of south Greenland glaciers to recent climatic change, Arct. Alp. Res., 24(2), 124–132, doi:10.2307/1551532, 1992.

Whiticar, M. J.: Carbon and hydrogen isotope systematics of bacterial formation and oxidation of methane, Chem. Geol., 161, 291–314, 1999.

Whiticar, M. J. and Schoell, M.: Biogenic methane formation in marine and freshwater environments: CO2 reduction vs. acetate fermentation- Isotope evidence, Geochim. Cosmochim. Acta, 50, 693–709, 1986.

Wimpenny, J., James, R. H., Burton, K. W., Gannoun, A., Mokadem, F. and Gíslason, S. R.: Glacial effects on weathering

https://doi.org/10.5194/tc-2020-155
Preprint. Discussion started: 3 July 2020

processes: New insights from the elemental and lithium isotopic composition of West Greenland rivers, Earth Planet. Sci. Lett., 290(3–4), 427–437, doi:10.1016/j.epsl.2009.12.042, 2010.

Wimpenny, J., Burton, K. W., James, R. H., Gannoun, A., Mokadem, F. and Gíslason, S. R.: The behaviour of magnesium and its isotopes during glacial weathering in an ancient shield terrain in West Greenland, Earth Planet. Sci. Lett., 304(1–2), 260–269, doi:10.1016/j.epsl.2011.02.008, 2011.

Winsor, K., Carlson, A. E. and Rood, D. H.: 10Be dating of the Narsarsuaq moraine in southernmost Greenland: Evidence for a late-Holocene ice advance exceeding the Little Ice Age maximum, Quat. Sci. Rev., 98, 135–143, doi:10.1016/j.quascirev.2014.04.026, 2014.

Yde, J. C., Knudsen, N. T., Hasholt, B. and Mikkelsen, A. B.: Meltwater chemistry and solute export from a Greenland Ice Sheet catchment, Watson River, West Greenland, J. Hydrol., 519(PB), 2165–2179, doi:10.1016/j.jhydrol.2014.10.018, 2014.

https://doi.org/10.5194/tc-2020-155
Preprint. Discussion started: 3 July 2020

The Cryosphere Discussions
Open Access
EGU

Table 1. Mineral weathering reactions and impacts on dissolved CO_2 concentrations.

Eq.	*Mineral*	*Acid*	*Abbreviation*[1]	*Reaction*	*Impact on CO_2*
(1)	Carbonate	Carbonic	$Carb_{CA}$	$(Ca, Mg)CO_3 + H_2O + \mathbf{CO_2} \rightarrow (Ca^{2+}, Mg^{2+}) + 2HCO_3^-$	CO_2 sink
(2)		Sulfuric	$Carb_{SA}$	$2(Ca, Mg)CO_3 + H_2SO_4 \rightarrow 2(Ca^{2+}, Mg^{2+}) + SO_4^{-2} + H_2O + \mathbf{CO_2}$	CO_2 source
(3a)	Silicate	Carbonic	Sil_{CA}	$(Ca, Mg)Al_2Si_2O_8 + \mathbf{2CO_2} + 3H_2O \rightarrow (Ca^{2+}, Mg^{2+}) + 2HCO_3^- + Al_2Si_2O_5(OH)_4$	CO_2 sink
(3b)				$(Na, K)AlSi_3O_8 + \mathbf{CO_2} + 5.5H_2O \rightarrow (Na, K) + HCO_3^- + 0.5Al_2Si_2O_5(OH)_4 + 2H_4SiO_4$	CO_2 sink
(4a)		Sulfuric	Sil_{SA}	$(Ca, Mg)Al_2Si_2O_8 + H_2SO_4 + H2O \rightarrow (Ca^{2+}, Mg^{2+}) + SO_4^{-2} + Al_2Si_2O_5(OH)_4$	No impact
(4b)				$2(Na, K)AlSi_3O_8 + H_2SO_4 + 9H_2O \rightarrow 2(Na^+, K^+) + SO_4^{2-} + Al_2Si_2O_5(OH)_4$	No impact

[1] Abbreviations are based first on the mineral class (carbonate = carb, silicate = sil) and then on the acid (carbonic acid = CA, sulfuric acid = SA)

https://doi.org/10.5194/tc-2020-155
Preprint. Discussion started: 3 July 2020

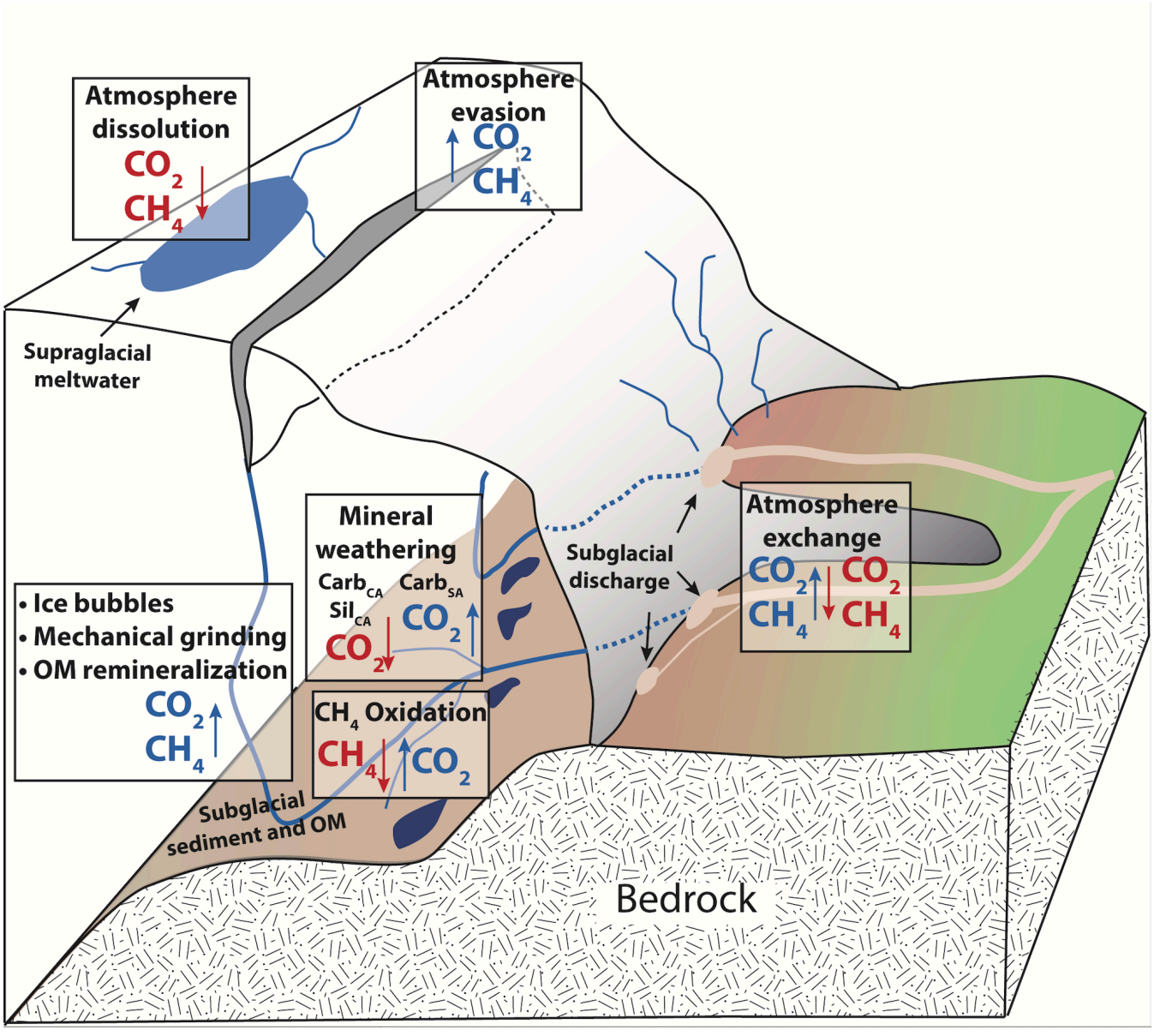

695 **Figure 1: Conceptual diagram of subglacial sources and sinks of CO_2 and CH_4. Arrow indicate the direction of fluxes. Boxes represent processes, and sources of gases to subglacial meltwaters are indicated by green text while sinks of gases to subglacial meltwater are indicated by red text. Gas bubbles, mechanical grinding, and OM remineralization are grouped because all are CO_2 and CH_4 sources.**

https://doi.org/10.5194/tc-2020-155
Preprint. Discussion started: 3 July 2020

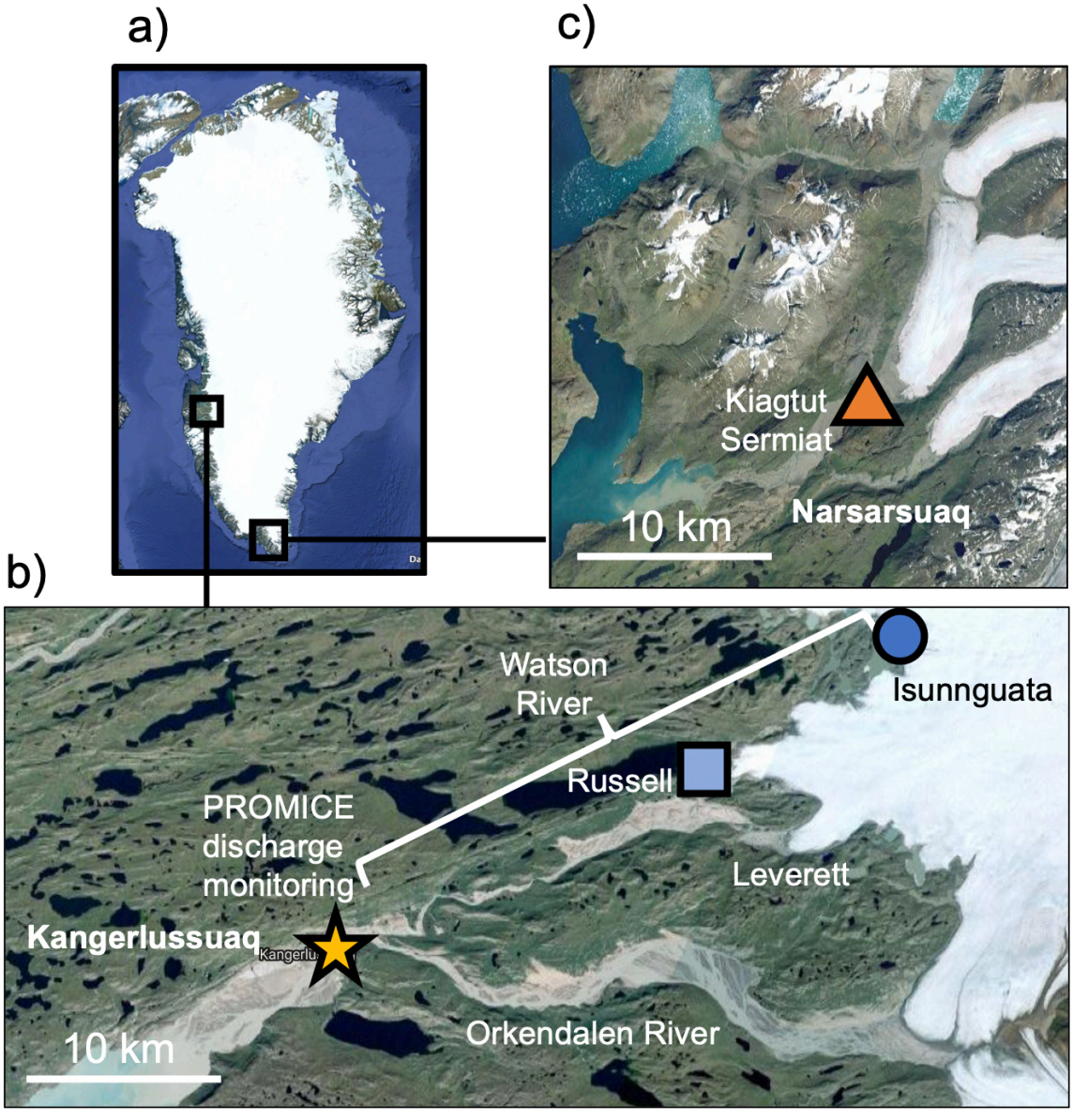

Figure 2. © Google Earth satellite images of study locations in a) Greenland including b) Isunnguata (dark blue circle) and Russell (light blue square) subglacial discharge sites flowing to the Watson River in southwest Greenland (c) and the Kiattut Sermiat site (orange triangle) in southern Greenland. Discharge monitoring of the Watson River is collected by PROMICE (van As et al., 2018) at the location represented by the yellow star.

https://doi.org/10.5194/tc-2020-155
Preprint. Discussion started: 3 July 2020

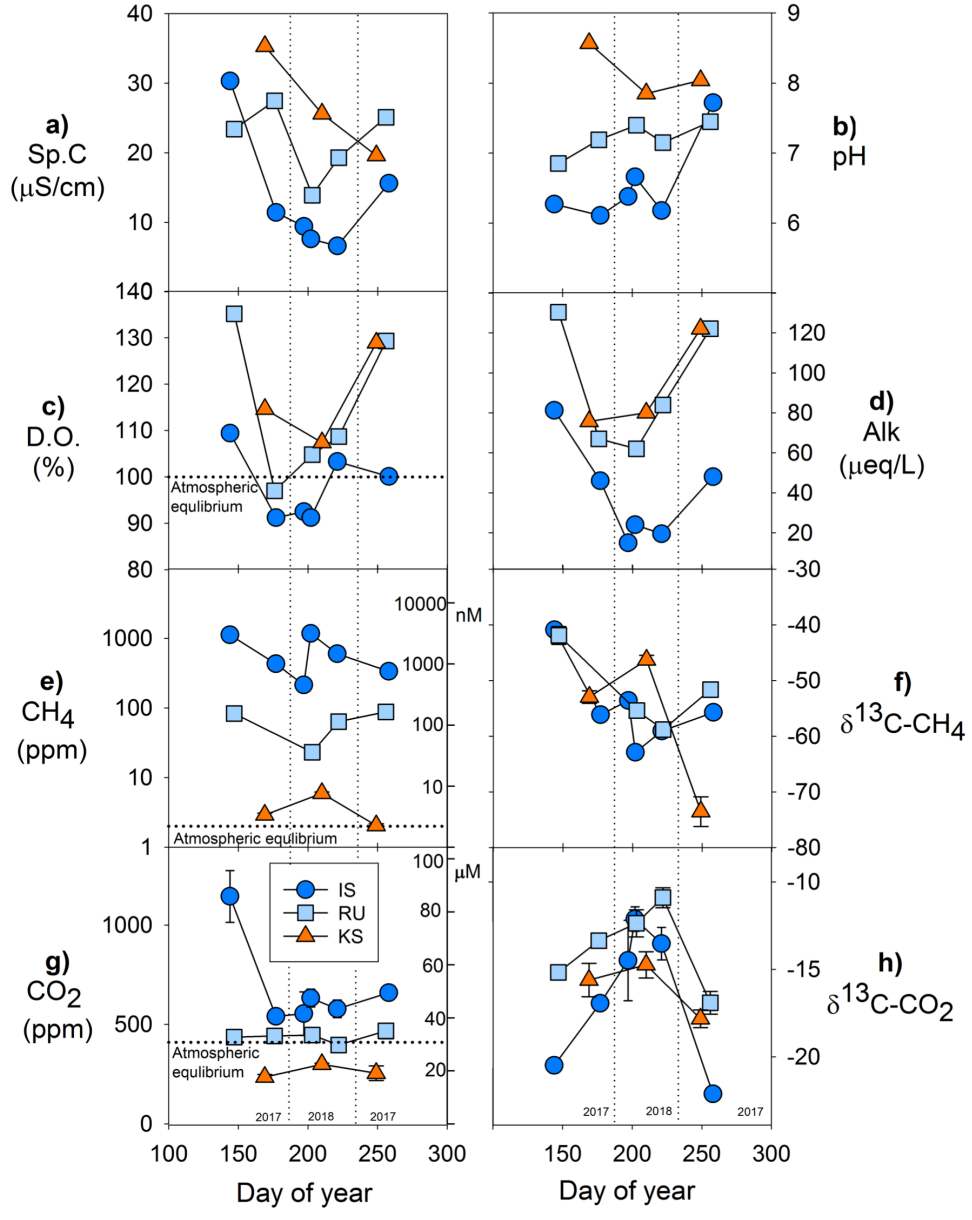

Figure 3. Chemical parameters at Isunnguata (IS), Russell (RU) and Kiattut Sermiat (KS) subglacial discharge sites versus day of year for a) specific conductivity (Sp.C), b) pH, c) dissolved oxygen (D.O.) percent saturation, d) alkalinity (Alk), e) measured CH_4 concentrations (left y-axis in ppm and right y-axis in nM), f) δ^{13}-CH_4 values, g) measured CO_2 concentrations (left y-axis in ppm and right y-axis in µM), and h) $\delta^{13}C$-CO_2 values. Atmospheric equilibrium concentrations are indicated by dashed lines and taken as 1.9 ppm for CH_4 and 410 ppm for CO_2. Error bars on CH_4 and CO_2 concentrations and stable isotopic compositions represents the standard deviation of replicates and are smaller than symbols for some data points.

https://doi.org/10.5194/tc-2020-155
Preprint. Discussion started: 3 July 2020

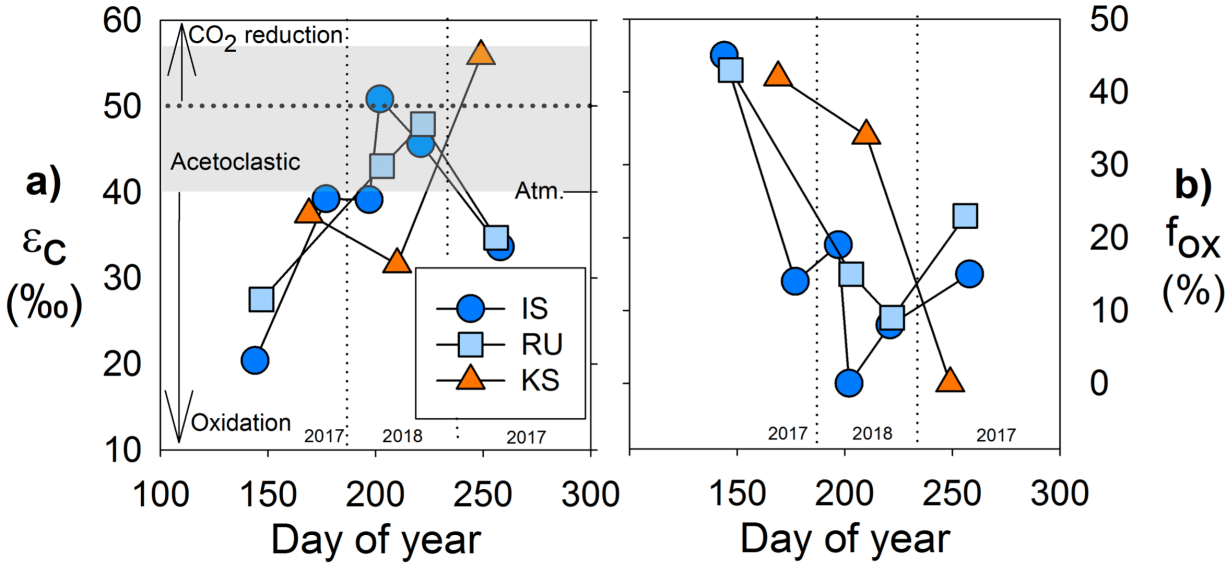

Figure 4. CH_4 dynamics over the course of the 2017 and 2018 melt seasons including a) the carbon fractionation factor (ε_c) between dissolved CO_2 and CH_4 and b) the fraction of CH_4 oxidized (fo_x) for Isunnguata (IS), Russell (RU) and Kiattut Sermiat (KS) samples. Fields of ε_c representing methanogenesis and oxidation values are based on Whiticar (1999). Values of ε_c between approximately 40 and 55 are produced for methanogenesis via acetate fermentation, while CO_2 reduction produces values between approximately 50 and 90. Lower values result from a predominant isotopic signature of CH_4 oxidation. Atmospheric input without additional alteration of CO_2 or CH_4 isotopic systematics results in a ε_c value of approximately 40.

https://doi.org/10.5194/tc-2020-155
Preprint. Discussion started: 3 July 2020

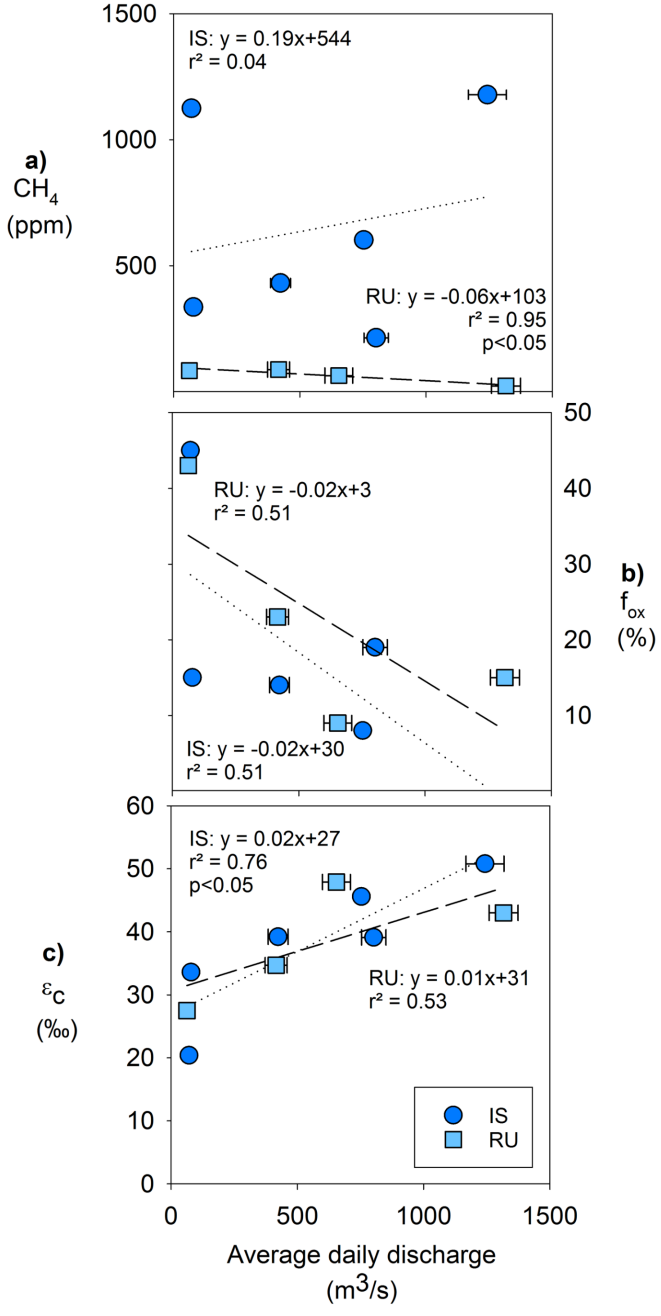

Figure 5. Discharge relationships with CH_4 dynamics including a) CH_4 concentrations, b) f_{ox}, and c) ε_c for Isunnguata (IS) and Russell (RU) samples. Regressions are shown by dotted lines for Isunnguata and dashed lines for Russell samples. Average daily discharge estimates are for the outlet of the Watson River and provided by PROMICE (van As et al., 2018). Horizontal error bars represent the standard deviation of average daily discharge for days samples were collected and are smaller than symbols for some data points.

https://doi.org/10.5194/tc-2020-155
Preprint. Discussion started: 3 July 2020

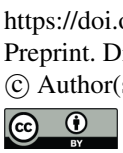

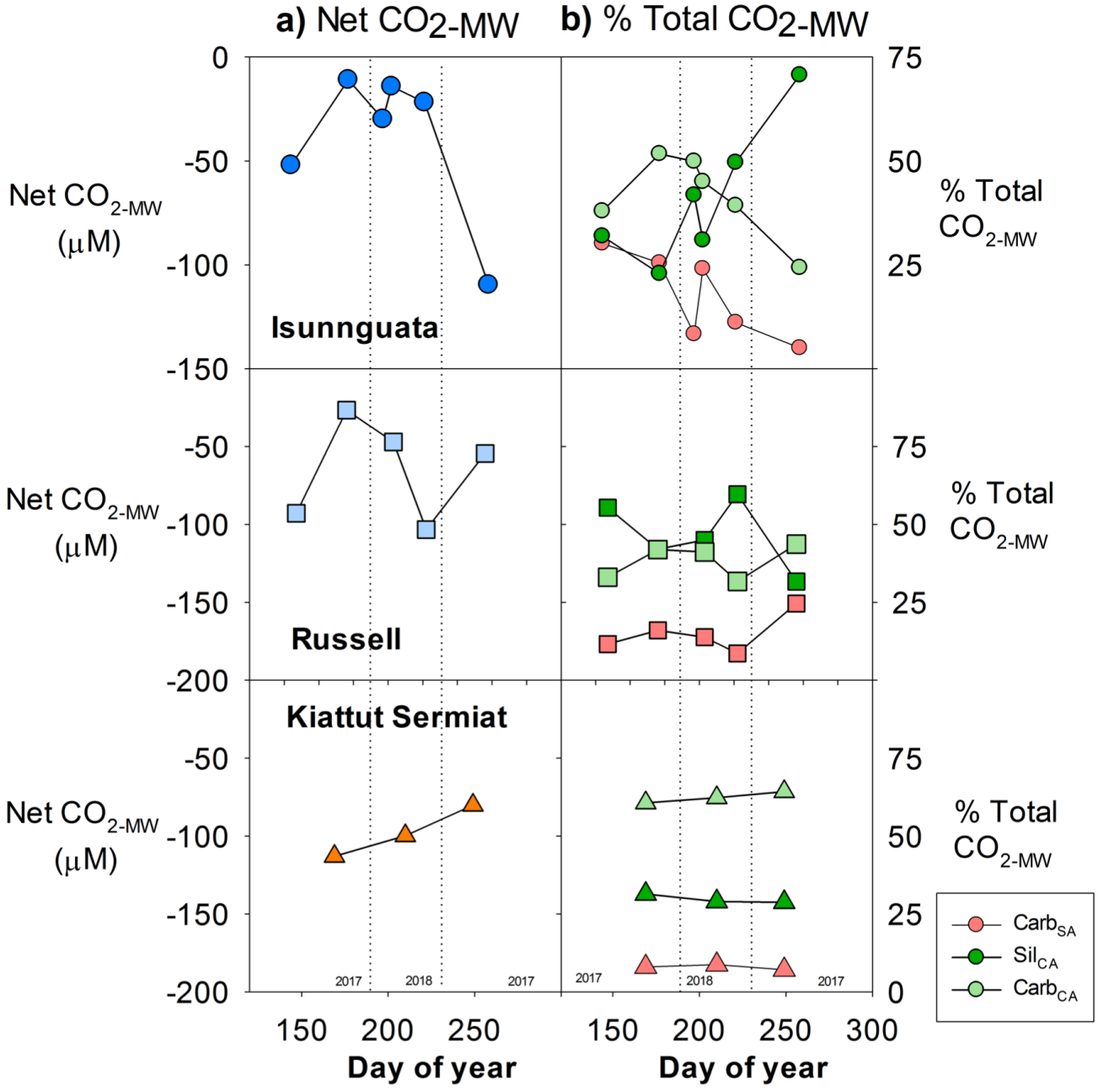

730 **Figure 6. Mineral weathering model results in a) net impact of mineral weathering reactions on CO_2 (Net $CO_{2\text{-}MW}$; Eq. 7) for Isunnguata, Russell, and Kiattut Sermiat subglacial discharge sites (where negative values of Net $CO_{2\text{-}MW}$ indicate net sequestration of CO_2 due to mineral weathering), and b) the proportional contribution of each mineral weathering reaction to the total change in CO_2 (% Total $CO_{2\text{-}MW}$ Eq. 9a-9c).**

https://doi.org/10.5194/tc-2020-155
Preprint. Discussion started: 3 July 2020

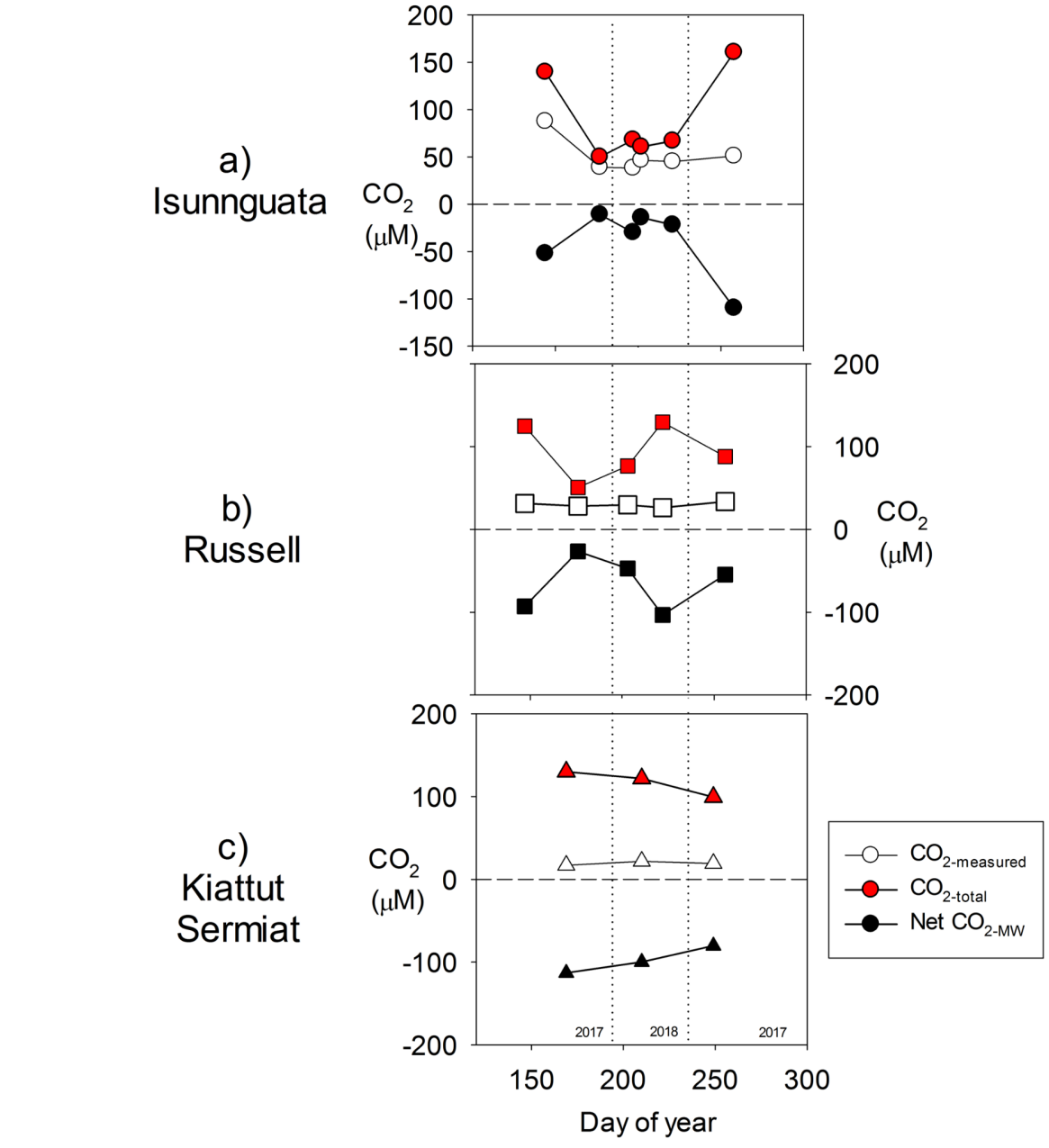

735

Figure 7. Calculated $CO_{2\text{-total}}$ values for a) Isunnguata, b) Russell, and c) Kiattut Sermiat subglacial discharge against day of the year.

https://doi.org/10.5194/tc-2020-155
Preprint. Discussion started: 3 July 2020

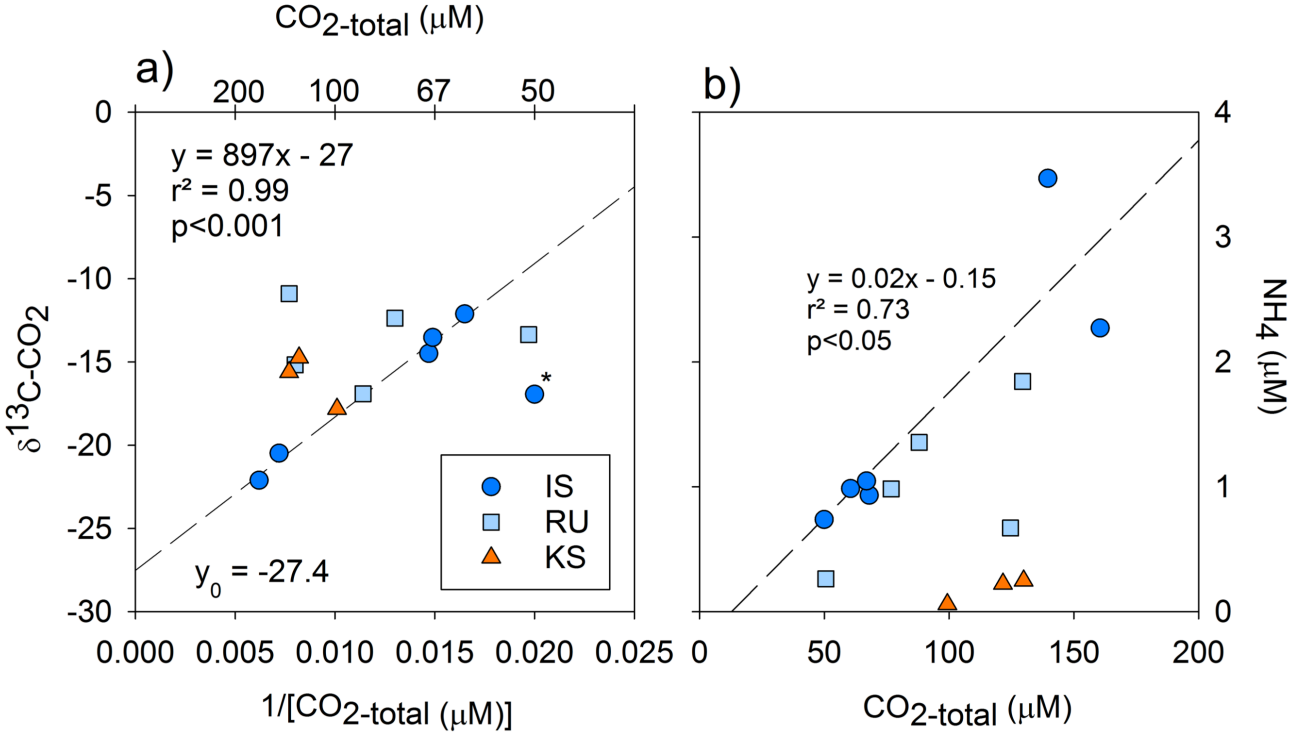

740

Figure 8. Correlations between the magnitude of $CO_{2\text{-total}}$ and a) $\delta^{13}C\text{-}CO_2$ and b) NH_4 for Isunnguata (IS), Russell (RU) and Kiattut Sermiat (KS) samples. Asterisk denotes the Isunnguata outlier not included in the regression between $CO_{2\text{-total}}$ and $\delta^{13}C\text{-}CO_2$ in panel a).

745

https://doi.org/10.5194/tc-2020-155
Preprint. Discussion started: 3 July 2020

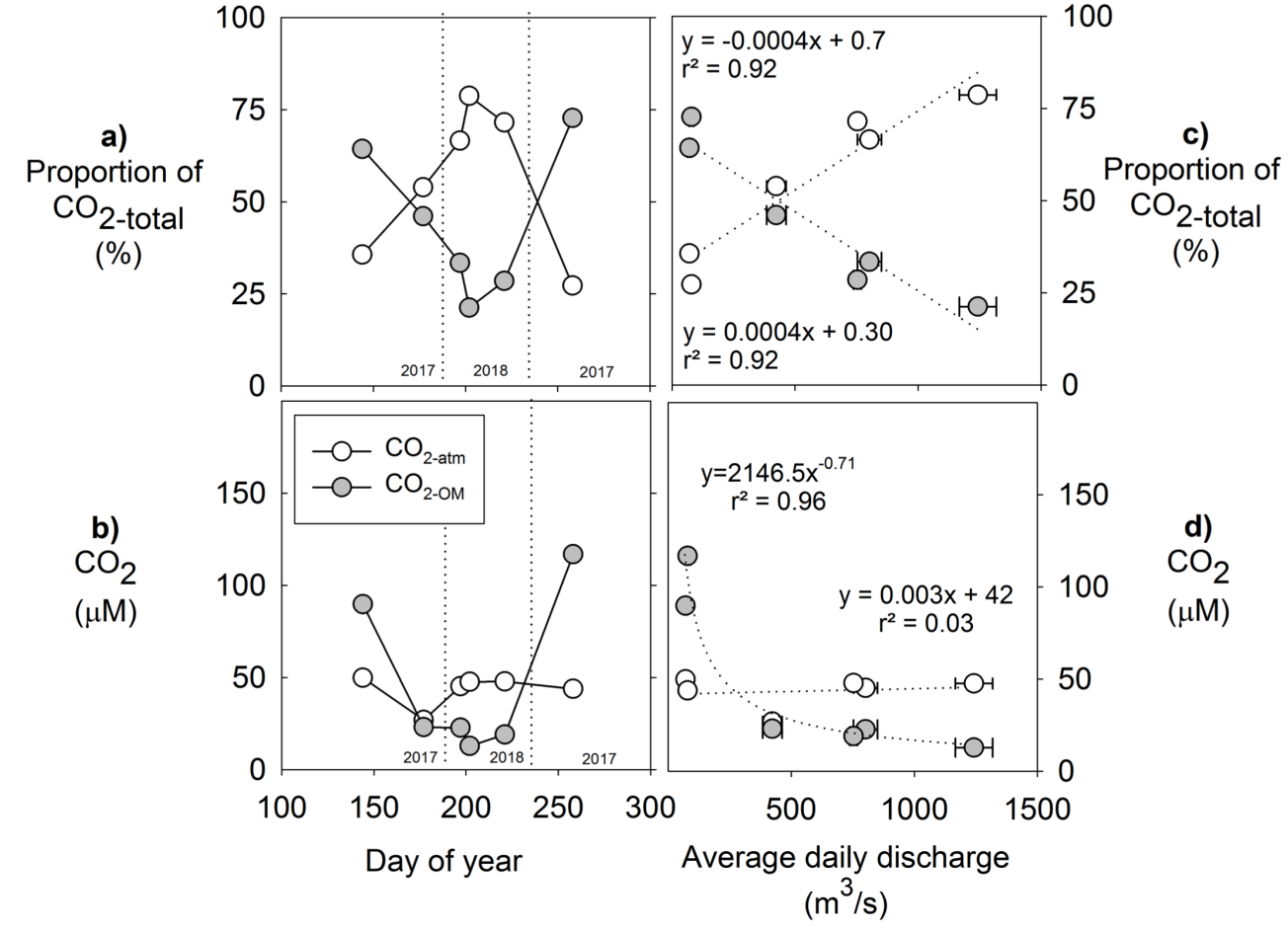

Figure 9. Estimates of contributions of atmospheric CO_2 ($CO_{2\text{-atm}}$) compared to that derived from remineralized OM ($CO_{2\text{-OM}}$) for Isunnguata subglacial discharge site including a) relative contributions according to the day of the year, b) absolute magnitudes according to the day of the year, c) relative contributions according to Watson River average daily discharge, and d) absolute magnitudes according to Watson River average daily discharge. Average daily discharge estimates are for the outlet of the Watson River and provided by PROMICE (van As et al., 2018). Horizontal error bars represent the standard deviation of average daily discharge for days samples were collected and are smaller than symbols for some data points. Regressions between average daily discharge and proportional and absolute contributions of $CO_{2\text{-atm}}$ and $CO_{2\text{-OM}}$ sources are shown with dotted lines.